esa

ECOSPHERE

Aggregative and feeding thresholds of sympatric rorqual whales within a fjord system

ERIC M. KEEN †

Scripps Institution of Oceanography, UC: San Diego, 9500 Gilman Drive, La Jolla, California 92093 USA

Citation: Keen, E. M. 2017. Aggregative and feeding thresholds of sympatric rorqual whales within a fjord system. Ecosphere 8(3):e01702. 10.1002/ecs2.1702

Abstract. Rorqual whales (f. Balaenopteridae) supposedly respond to increases in prey supply according to both aggregative and feeding thresholds. With the former, they gather in areas above a minimum prey density set by their basal metabolic needs. With the latter, feeding occurs only above a prey density set by the energetic cost of lunge feeding. To compare prey preferences and the two threshold types in sympatric rorquals, I conducted systematic transect surveys and behavioral observations of humpback whales (*Megaptera novaeangliae*) and fin whales (*Balaenoptera physalus*) in a British Columbia fjord system. While multiple prey features were found to influence whale aggregation and feeding, both threshold types were observed in each species' response to krill volume. Humpback response to prey features was less predictable and influenced by more factors than that of fin whales, which appeared to be exclusively euphausivorous and interested in the deepest high-volume krill patches within the deepest channels. Compared with fin whales, humpbacks found higher-volume krill patches and had higher aggregative thresholds, but had lower feeding thresholds. Findings aligned overall with the expectations that aggregative behavior is responsive to local prey supply, while feeding thresholds are governed by less mutable energetic constraints imposed by body size and feeding mode. Both aggregative and feeding threshold responses appeared to be a function of local conditions: As total krill-like backscatter increased, feeding thresholds stabilized (became more nonlinear and more nonrandom), while aggregative thresholds destabilized. All results emphasized the importance of incorporating observations of feeding effort in studies of prey preference and habitat use.

Key words: aggregative threshold; *Balaenoptera physalus;* baleen whales; feeding threshold; fin whale; fjord; foraging strategy; humpback whale; *Megaptera novaeangliae;* rorqual; threshold foraging.

Received 1 November 2016; revised 7 January 2017; accepted 12 January 2017. Corresponding Editor: Hunter S. Lenihan.

† **E-mail:** ekeen@ucsd.edu

INTRODUCTION

During the foraging season, whale distribution and behavior are closely coupled to those of their prey (Berta et al. 2006). Hollings (1965) provided a formal framework for the varieties of functional response of predators to changes in prey supply. His type III S-curve represents a density-dependent "threshold" response, in which the proportion of prey destroyed initially increases nonlinearly with prey density until an inflection point is reached, above which the proportion destroyed declines asymptotically. Parker and Boseman (1954) proposed an energetic mechanism for threshold response, suggesting that the basking shark (*Cetorhinus maximus*) would be "feeding at a loss" (Sims 1999) unless it maintained a close association with areas with anomalously high zooplankton density. Foraging thresholds are expected to be high for sharks, whales, and other pelagic predators because the metabolism and mobility essential to their life strategies in water require activity levels and body plans that are energy intensive to maintain

(Alexander 2005). Mobility is thus double-edged, conferring access to a larger foraging area but reducing the proportion of usable area above the profitability threshold.

Aggregative thresholds, in which predator densities change in response to prey densities in a type III curve, have been documented in several taxa and systems: waterfowl (van Eerden 1984, Mitchell et al. 1994, De Leeuw 1999, Lovvorn et al. 2013), coastal benthic systems (Hines et al. 1997, Seitz et al. 2008), terrestrial systems (Forcardi et al. 1996), sharks (Parker and Boseman 1954, Sims 1999), and seabirds (Piatt 1990). Many studies of aggregative response have aligned well with the predictions of energetic models (Lovvorn and Gillingham 1996, Sims 1999, Sponberg and Lodge 2005, Nolet et al. 2006, but see Lovvorn et al. 2013). Predators can aggregate for reasons unrelated to foraging, such as reproduction or safety from other predators, but here my scope is restricted to aggregative foraging response.

That baleen whales associate with very dense prey patches is a common finding (Dolphin 1987, Mayo and Marx 1990, Croll et al. 2001, 2005, Friedlaender et al. 2006, Witteveen et al. 2008, Goldbogen et al. 2011), but Piatt and Methven (1992) was the first of only two studies to observe threshold aggregative response in a whale species (in their case, the humpback, *Megaptera novaeangliae*) to increasing prey (capelin, *Mallotus villosus*) within a defined area (Witless Bay, Newfoundland). The other study is Feyrer and Duffus (2015; gray whales, *Eschrictius robustus*, feeding upon mysids, f. Mysidae, off west Vancouver Island). Recent models of whale–prey association have found nonlinear relationships in their model output that are suggestive of nonlinear and sigmoid- or Hollings-type responses (Friedlaender et al. 2006, Keen et al. 2017).

Feeding thresholds may also apply to certain marine predators. Aggregative thresholds govern predator position with respect to available prey, at which point a predator must decide whether or not to feed. The lunge feeding mode of rorqual whales (f. Balaenopteridae) distinguishes these predators, the ocean's largest, from other filter feeders such as right whales and from other marine homeotherms such as seabirds. The energetic costs of lunge feeding are extreme (Goldbogen et al. 2007), and theoretically, they combine with the inherently high metabolic needs of rorquals to set superlative feeding thresholds (Goldbogen et al. 2011). However, published examples of whales are few (North Atlantic right whales, *Eubalaena glacialis*, Mayo and Marx 1990, gray whales, Feyrer and Duffus 2015), which could be due either to the complex study design needed to identify them or to the conflation of the two threshold types in the literature.

Comparing aggregative and feeding thresholds is even more difficult, since prey sampling near feeding predators must occur during systematic, scale-appropriate surveys of predator and prey within a defined area. Feyrer and Duffus (2015) were the first to attempt this comparison. The two threshold types need not occur at the same prey densities, though they may be related. If the energetic cost of feeding is negligible (e.g., passive filter feeding while traveling; Goldbogen et al. 2017), energy deficits can be partially offset even in areas with sub-threshold prey densities, thus increasing the chances of satiation once adequate patches are found. But when the act of feeding is costly, as in the case of rorquals, starving may be more energy conserving than feeding. It follows that feeding thresholds should occur at different prey densities than aggregative thresholds in certain taxa, with potentially profound ecological implications (Solomon 1949, Hollings 1965, Hassell and May 1974, Abrams 1983). Aggregative thresholds may also be context dependent, such that threshold height changes as a function of prey supply and ecosystem state (Piatt 1990, Piatt and Methven 1992, Feyrer and Duffus 2015). In contrast, a feeding threshold response is a binary behavioral shift (feeding or not) defined by inherent energetic constraints that should not be context dependent (though this has never been shown). Differences in the height of the two threshold types should influence predator–prey dynamics and other ecological processes, but these concepts remain largely theoretical, highlighting the need for studies that observe both threshold types simultaneously.

Aggregative and feeding thresholds also have consequences for the conservation and monitoring of marine predators, since predators may appear spatially and behaviorally decoupled to prey and the habitat drivers of prey when prey

densities are far below or far above the vicinity of the threshold. In efforts to identify habitats critical to the recovery of threatened marine predators, it is paramount to understand the dynamics of threshold foraging behavior in a given study site. The recent return of recovering humpback and fin whale (*Balaenoptera physalus*) populations to a fjord system in northern British Columbia, where they had been severely depleted by industrial whaling (Ford 2014), presents an opportunity to compare the relationship between aggregative and feeding thresholds in two rorqual species within a relatively confined and unique marine habitat. Using an ecosystem sampling design that combines systematic surveys with close observations of whales, I first sought to understand which prey-related habitat features govern the spatial pattern and feeding effort of each species. Second, within this broad context of whale–prey interactions, I sought to identify, characterize, and compare aggregative and feeding thresholds. Third, I sought to ascertain the context dependence of whale–prey associations and both threshold types. Throughout, I sought to meet these objectives using analytical approaches that were sensitive to the multiple spatial and temporal scales involved.

Methods

Study area

Geography.—The study area (1961 km^2 of water) is located within the marine territory of the Gitga'at First Nation in the Kitimat Fjord System (KFS) of northern mainland British Columbia, centered at 53° N and 129° W (Fig. 1). This fjord complex extends 140 km inland from the Pacific Coast (MacDonald et al. 1983), nested within the Great Bear Rainforest, a segment of the largest temperate coastal rainforest in the world (Thompson 1981). Marine habitat in the KFS is shaped by processes typical of fjord oceanography: estuarine circulation (forced by freshwater discharge), wind forcing (e.g., katabatic outflows), and dramatic tides (reviewed in Keen 2017*a*).

Whales and diet.—Industrial whaling severely depleted humpbacks and fin whales from the coastal fjords of British Columbia, Canada (Ford 2014), but as their North Pacific populations recovered, they began returning en force in the last two decades (Gregr et al. 2006, Ashe et al. 2013, FOC 2013, Ford 2014; L. Nichol, *personal communication*). In the spring, seasonally resident humpbacks migrate to the KFS from tropical Pacific breeding grounds, primarily Hawaii (Barlow et al. 2011, Ashe et al. 2013). Most leave the KFS by late fall. During the summer, these humpbacks feed opportunistically upon euphausiids and small schooling fish. Based on field observations and local traditional knowledge, fish prey include herring (*Clupea harengus pacifica*), sand lance (*Ammodytes hexapterus*), sardine (*Sardinops sagax caerulea*), and various species of smelt (f. Osmeridae).

During British Columbia's commercial whaling period, fin whales were predominantly hunted in British Columbia's offshore waters past the continental shelf, though 17% of British Columbia fin whale kills between 1908 and 1967 (for which location information is available) took place on the continental shelf in exposed coastal areas (e.g., Hecate Strait and Queen Charlotte Sound) and several confined waterways along the north-central mainland British Columbia coast (COSEWIC 2005, Gregr et al. 2006). Of these confined waters, none were more frequented by fin whales than the waters of the KFS (DFO Cetacean Research Program, *unpublished data*). Along with fin whales elsewhere in British Columbia, the population was decimated in the KFS by whaling, and only a handful of alleged sightings occurred in KFS waters between 1968 and 2006, after which fin whales began occurring regularly within the KFS once again (Ford 2014). They have been increasing steadily there ever since (L. Nichol, *personal communication*).

The majority of North Pacific fin whale diet studies are based on stomach analyses of flensed whales and pertain to regions further offshore or north of British Columbia (Pike 1950). Stomachs contained mainly (sometimes exclusively) euphausiids in these studies, but the proportion of diet components could change significantly between years (Flinn et al. 2002). Other prey species include copepods, fish, and cephalopods. The euphausiids preyed upon by fin whales included *Euphausia pacifica*, *Thysanoessa spinifera*, *T. longipes*, and *T. inermis* (Flinn et al. 2002).

Data collection

In the summers of 2014 and 2015, whale and ecosystem surveys were conducted aboard the

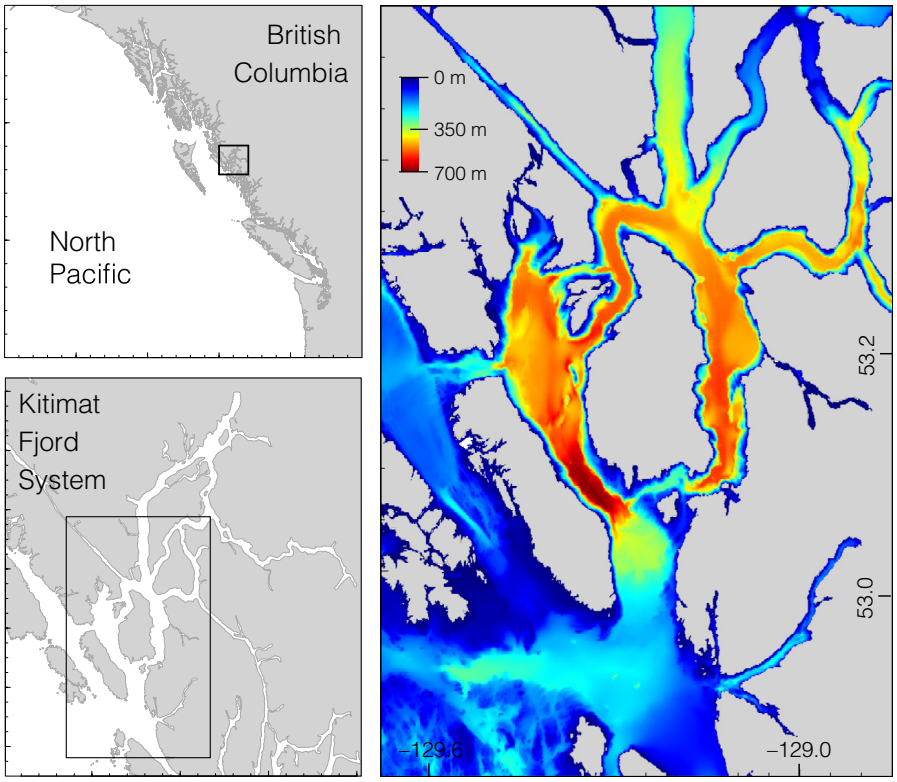

Fig. 1. Study area within the Kitimat Fjord System, Gitga'at First Nation territory, British Columbia, Canada. Colors portray seafloor depth.

RV Bangarang, a 12-m motorsailer, with a team of three researchers. Circuits of the study area were completed within a target duration of 20 d, during which we visited a grid of oceanographic stations (n = 24), between which we conducted concurrent visual and acoustic transect surveys. Data (Keen 2017*b*) were collected over 155 d throughout the summers of 2014 and 2015, during which 2291 km of transect surveys was completed (Table 1, Fig. 2). Mean survey duration was 22 d, 313 km. Two surveys were completed during August–September 2014, and five surveys were completed during June–September 2015.

Visual surveys for whales and debris.—Whale surveys were carried out using line-transect sampling methodology (Buckland et al. 2001). Bearing and reticle readings using Fujinon 7 × 50 binoculars, min-max-best group size estimates, and cue behaviors for each sighting were recorded by an observation team from a platform 2 m above sea level. Whale positions were geo-located using binocular bearing and reticle readings from the observation platform (using R package *bangarang*, which accounts for horizon obstruction in confined North Pacific channels). Visual effort yielded 1688 whale sightings (1529 humpbacks and 159 fins; Table 2, Fig. 3).

Table 1. Fieldwork synopsis for data collection aboard the *RV Bangarang*, detailing the duration of monthly surveys (d), kilometers of transect effort (km), and the average Beaufort sea state (Bft).

		Surveys		
Year	Month	Days	km	Bft
2014	August	19	265	1.4
	September	19	273	1.2
2015	May–June	16	320	1.6
	June–July	26	335	1.3
	Late July	21	346	1.4
	August	26	322	1.4
	September	28	330	1.4
	Total	155	2191	

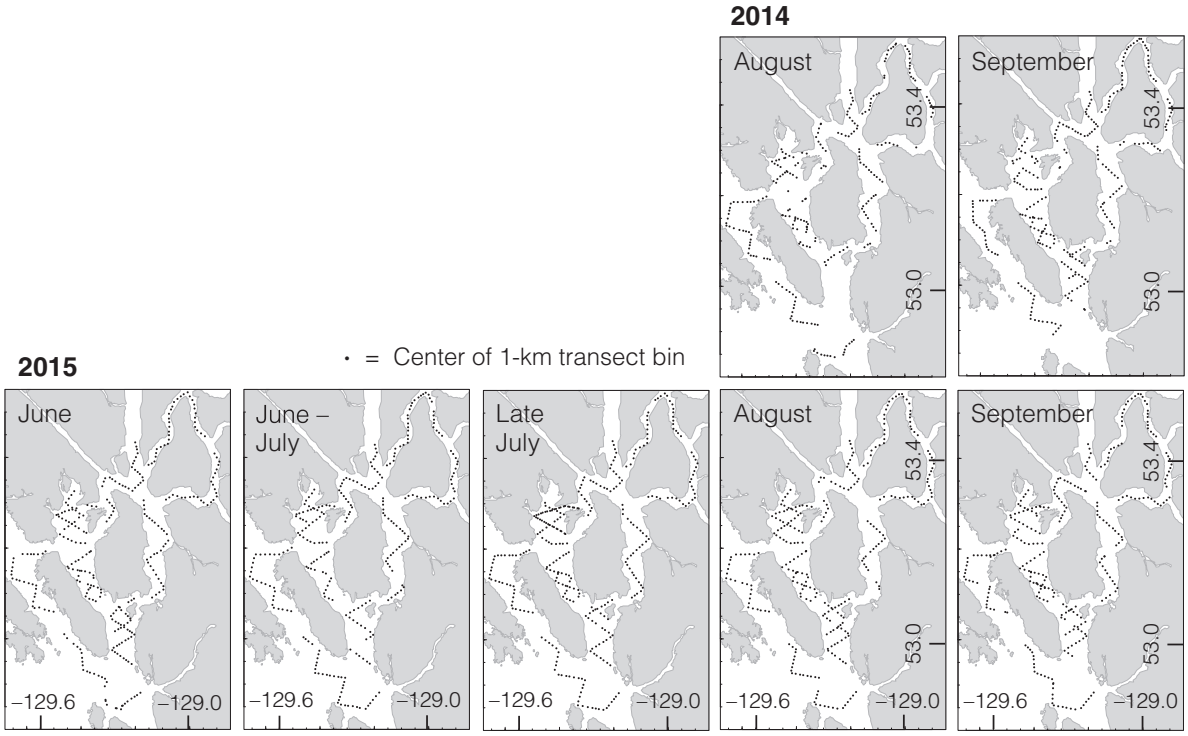

Fig. 2. Systematic transect effort. Each dot is the geographic centroid of a 1-km segment of hydroacoustic transect.

Aggregations of surface debris, ubiquitous within fjord systems, serve as indicators of tidal mixing and internal wave activity that can aggregate nutrients and plankton and attract nekton (Wolanski and Hamner 1988) and predators including rorqual whales (Chenoweth et al. 2011). During fieldwork, we found anecdotally that whales were regularly associated with areas of dense debris. To gauge the role of fjord currents in whale–prey associations, we quantified debris densities by conducting concurrent strip-width surveys using standard strip-transect methodology typical of seabird surveys (Buckland et al. 2001). The survey strip was 150 m on each side of the vessel (300 m in total), broken into two zones (0–75 and 75–150 m) gauged using handheld rangefinders designed for confined channels (Keen et al. 2016). All types of surface debris were noted, as well as zones of water mixing and surface signatures of internal waves (collectively referred to as "Beaufort belts" or BFT belts).

Acoustic backscatter.—Hydroacoustic data were collected with a down-sounding *Syqwest Hydrobox* echosounder (33 and 200 kHz dual frequency) to obtain a profile map of the ambient depth, distribution, and patchiness of backscatter down to 300 m, a range that encompasses the maximum dive recorded for humpback whales (Hamilton et al. 1997) and the common dive range for fin whales (100–230 m; Leatherwood and Reeves 1983, the maximum recorded dive depths, 470–565 m, were observed in Mediterranean fin whales; Notarbartolo-di-Sciara et al. 2003, Panigada et al. 2003). A preliminary study in 2013, with a 500-m backscatter range, did not detect any euphausiid-like backscatter below 250 m (Keen 2017*a*). Details of echosounder data collection and processing are provided in Keen et al. (2017).

Zooplankton tows.—Three daytime, plummet-style zooplankton tows (333 μm, 0.7 m diameter, OAR 6:1, flowmeter-equipped, dropped to 250 m; designed according to Keen 2015) were taken at the stations within each channel. Samples were immediately preserved in 5% formalin–seawater solution. Euphausiids were identified to species level by collaborators at Oregon State University (Bernard lab). Preliminary analysis of local net tows indicates that euphausiid species

Table 2. Whale sightings and focal follows.

			Sightings			Focal follows			
			Effort			Behavior			
Year	Leg	Species	Transect	Other	Total	Feed	Other	All	km
2014	All	Humpback	212	283	495	56	60	106	1.11
		Fin	34	35	69	12	12	24	2.31
	1	Humpback	121	194	315	37	35	72	1.09
		Fin	26	24	50	8	9	17	1.94
	2	Humpback	91	89	180	19	25	44	1.13
		Fin	8	11	19	4	3	7	3.23
2015	All	Humpback	416	618	1034	104	118	222	0.99
		Fin	42	48	90	19	7	24	2.46
	1	Humpback	61	89	150	21	24	45	1.22
		Fin	3	8	11	3	1	4	2.90
	2	Humpback	69	108	177	26	25	51	1.16
		Fin	0	7	7	3	1	4	2.07
	3	Humpback	78	70	148	16	16	32	1.04
		Fin	5	13	18	4	2	6	3.45
	4	Humpback	127	214	341	21	36	57	0.78
		Fin	17	8	25	3	2	5	2.01
	5	Humpback	81	137	218	20	17	37	0.76
		Fin	17	12	29	4	1	5	1.70
Grand total		Humpback	628	901	1529	160	178	338	1.03
		Fin	76	83	159	31	19	48	2.39
		All	704	984	1688	191	197	386	1.20

Notes: Sightings are number of individuals seen, reported according to observation effort at time of sighting (transect or other). Focal follows are reported according to the whale's inferred behavioral state. Column km reports average kilometers covered by vessel during focal follows.

present include, in descending rank of abundance, *E. pacifica* (by far), followed by *Thysanoessa*, then *T. gregaria* and *T. longipes* (K. Qualls, *personal communication*). *Tessarabrachion oculatum* is also present but extremely rare. Other zooplankton taxa dominated samples numerically, particularly copepods, amphipods, and chaetognaths. Detailed results will be published separately.

Focal follows.—When whales were seen, transect effort was suspended if possible and focal follows were attempted. Focal follow effort commenced once the vessel was within 150 m of the animals. Target duration was 5–15 min (1–3 km). While behavioral observations were being recorded, the vessel collected acoustic backscatter by tracing the whales' track at a distance of 100–150 m, moving from fluke footprint to footprint in a "mini-zigzag" pattern to achieve a broad sample of the prey field below the group. This zigzag pattern was adjusted as needed to minimize disturbance to the animals, position the observers for identification photographs, and avoid obstacles such as debris and the shore.

Group behavioral state was inferred during the focal follow and recorded along with a confidence level (95%, 66%, or 33%). Behaviors were assigned without knowledge of echosounder backscatter levels. Details of behavioral inference are provided in Keen (2017*a*).

We completed 388 focal follows (338 humpbacks, 50 fins; Table 2). Mean focal follow track length was 1.20 km (1.03 km for humpbacks, 2.39 km for fins); 49% of focal follows were of feeding whales (47% for humpback, 62% for fins). Focal follow locations were a representative sample of whale distribution found during surveys (Fig. 3).

Data preparation

Acoustic backscatter.—Acoustic backscatter processing is detailed in Keen et al. (2017). In summary, the *Syqwest Hydrobox* outputs a pixelated representation of water column backscatter. These pixel data were georectified to account for variable vessel speed and were visually scrutinized to ensure all reflections attributable to seafloor,

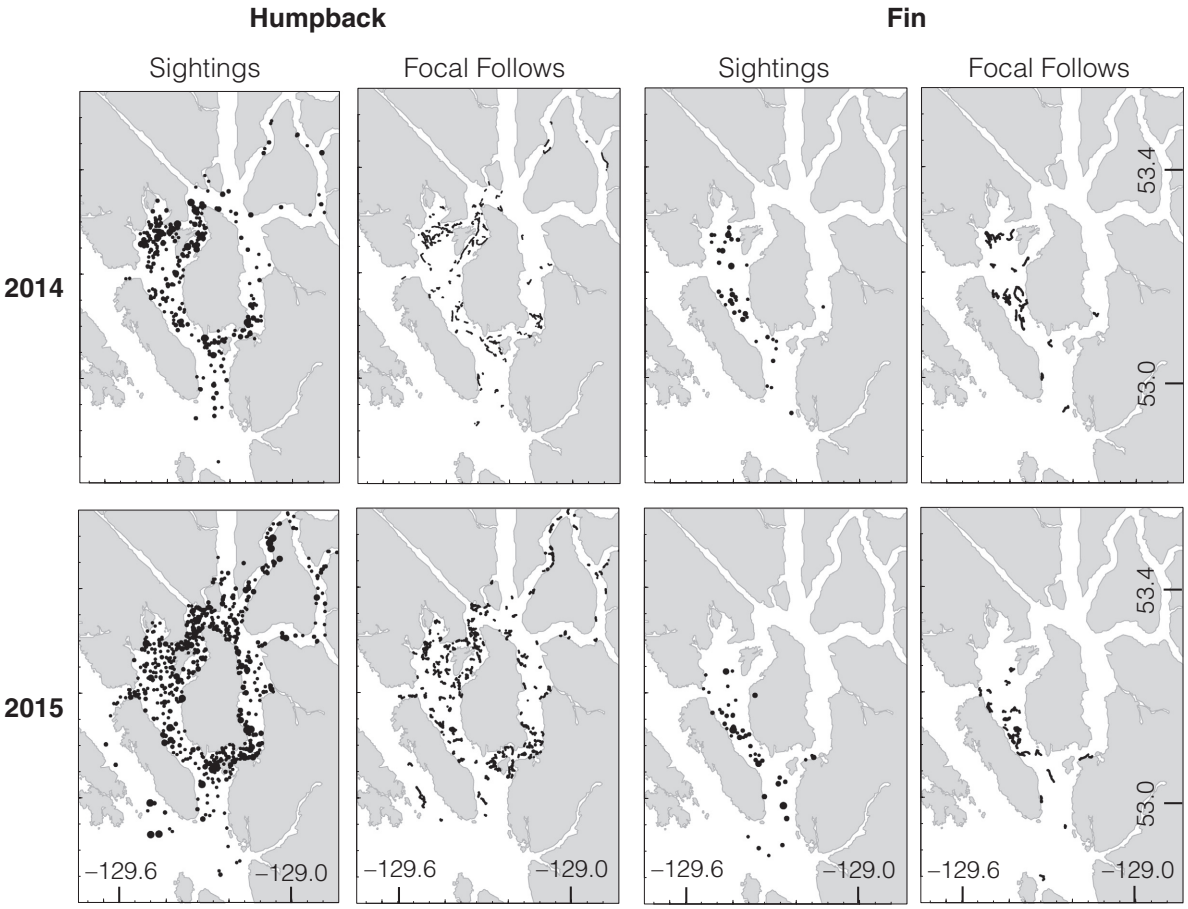

Fig. 3. Locations of whale sightings (all effort) and focal follows in 2014 (top) and 2015 (bottom) for humpbacks (left) and fin whales (right).

near-surface water bubbles, propeller cavitation, sonars of passing ships, and whales were removed. In order to reduce each frequency further to display only backscatter of probable whale prey, we filtered data based on patch characteristics and overlapping frequencies so that, to the extent possible, 33 kHz backscatter represents small schooling fish, while 200 kHz backscatter represents euphausiids (Fig. 4; see details in reference above for justification). Deepwater krill imaging and zooplankton tows were used to verify the efficacy of 200 kHz backscatter processing methods (Keen et al. 2017).

Middle-priced echosounders like that used in this study can characterize prey-like backscatter, but cannot quantify the biomass of constituent taxa. We developed four simple metrics for each filtered frequency, described below and depicted in Fig. 4. These metrics were cross-checked pairwise for collinearity.

1. Total backscatter (T): the mean sum of pixel values of prey-like backscatter; this is a proxy for the quantity of potential prey available. Total backscatter was log-transformed for all analyses; values that were originally 0 were assigned a post-transform value of −1.
2. Backscatter intensity (I): the mean pixel value of prey-like backscatter; this is a proxy that can represent the school density, body size and composition, and/or patch characteristics of potential prey swarms.
3. Mean depth (Z): the mean of the depth distribution of prey-like backscatter.
4. Vertical dispersion (D): the standard deviation of the depth distribution of prey-like

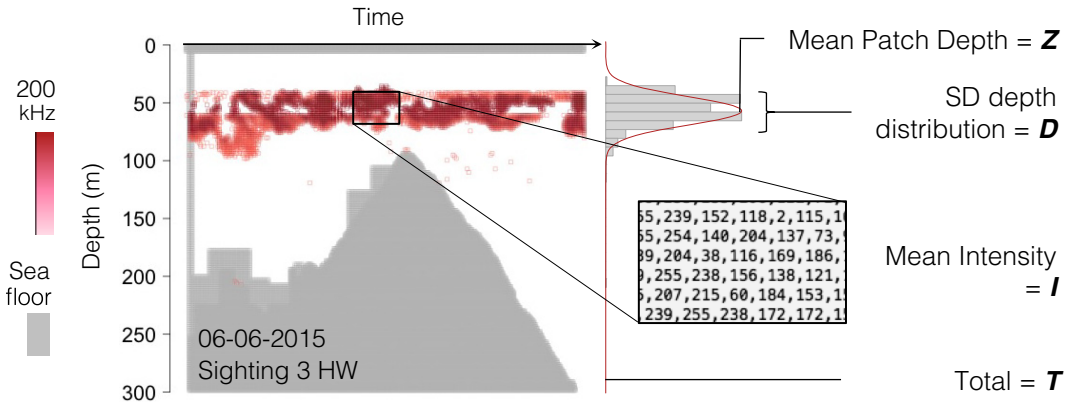

Fig. 4. Metrics used to characterize acoustic backscatter. Bottom to top: Total backscatter (*T*) is the sum of all backscatter registering above a manually set threshold, divided by the number of pings occurring within the focal follow. Mean intensity (*I*) is the mean value of those pixels. Dispersion (*D*) is the standard deviation of the depth distribution of pixels. Mean patch depth (*Z*) is the mean of that distribution. *y*-Axis is depth (m), *x*-axis is chronological order of echosounder pings georectified into 10-m horizontal bins, and backscatter is displayed on a red color gradient (deeper red = higher backscatter return; gray = seafloor or manually removed self-noise). Backscatter is stored as rows (pings) of 200 columns of pixel values (each pixel representing backscatter within a 1.5-m vertical bin; box inset). Example shown is from a focal follow of a humpback (sighting 03 on 6 June 2015).

backscatter; this is a proxy for the vertical extent of prey swarms; highly dispersed backscatter may be less ideal for batch-feeding predators such as rorqual whales.

Systematic echosounder transects were binned into segments (Fig. 2) of approximately 1.2 km (the average distance covered during echosounder sampling in focal follows; Table 2). Backscatter metrics were computed for each transect bin.

Behavior designation.—For analyses, the behavioral states recorded during focal follows were pooled into two categories: Feeding (defined as those inferred to be feeding with confidence level of 66% or higher) and Other (all other behaviors and confidence levels). Focal follow echograms were reviewed and the apparent predominant prey type present was recorded as "none," "krill," "fish," or "both." If classified as "none," the behavior for the followed whale was changed to "Other"; this step was taken to ensure that results reflected whale–prey interactions rather than data entry prowess. Prey-type designations were also used to modulate behavioral designations according to the backscatter frequency of interest in prey preference analyses; feeding whales whose backscatter was prey type "fish" were designated as behavioral state "Other" for analyses of 200 kHz backscatter metrics, and vice versa. Behavior for focal follows with prey type "both" remained unchanged. This modulation was not done for spatial distribution analyses such as aggregation generalized additive models (GAMs) and "position curves" (step 5 in *Analysis*).

Analysis

Analysis was driven by two primary questions: Which prey conditions are whales targeting? And, do whales exhibit threshold responses to changes in those conditions?

Targeted prey conditions.—1. Aggregative relationship to prey conditions.—We used GAMs to elucidate associations between whale aggregations and prey-related habitat features sampled during systematic transect surveys. The GAM is a modeling approach that relates observations (in our case, whale counts) to predictor variables using nonlinear link functions (smoothing or "spline" functions) without imposing parametric limits on the data (Hastie et al. 2009). generalized additive models can accommodate highly nonlinear functional relationships (Zuur et al. 2009). Generalized additive models were built using package *mgcv* (Wood 2011) in R.3.1.2 (R Core Team 2013; code for this study: Keen 2017*b*) with gamma set to 1.4 to prevent over-specification (Wood 2011).

Poisson, quasi-Poisson, and negative binomial models were explored (with their default link functions) for modeling whale counts on each effort segment.

The study area was split into 26 strata (after Keen et al. 2017), such that there were 26 data points for each of seven surveys (two in 2014 and five in 2015; $n = 159$). "Prey conditions" were represented using acoustic backscatter metrics and physiographic variables that may influence prey aggregation (seafloor depth and slope and evidence of tidal fronts). Models were built by adding single explanatory variables at a time, building off variable combinations that yielded the lowest corrected Akaike's information criterion (AICc; Akaike 1974, Burnham and Anderson 2002) and repeating until AICc no longer improved. Due to our sample size, models that were within six AICc of the lowest AICc were considered to be of equivalent fit (Hilbe 2011).

2. Context specificity of aggregative response.—To determine whether whales are aggregating according to the absolute or relative quality of these features, three versions of the data were fitted to whale counts: absolute conditions (no scaling), conditions scaled by the median of conditions (50th quantile) available during their respective survey months, and conditions scaled by the "best" available conditions (defined here as the 95th quantile for a given survey). AICc was used to determine which data scaling yielded the most explanatory model.

3. Associated prey conditions.—Environmental sampling during focal follows allowed us to determine the prey-related habitat features resulting from the aggregative behavior surveyed from transects. In addition to visual comparison of sample distributions, the Kolmogorov–Smirnov test (K–S test, Chakravarti and Roy 1967) was used to identify significant differences between prey-related conditions sampled near humpbacks and those near fin whales. Kolmogorov–Smirnov tests were used to compare behavioral states, "Feeding" and "Other," in each species and between species. Species were also compared without distinguishing behavioral states. One-sided tests evaluated the hypotheses that fin whales, being the larger of the two species with greater overall metabolic needs, were found among backscatter with higher total backscatter and higher intensity, concentrated in vertically compact patches (i.e., lower dispersion), at greater depths (based on the pattern that larger species target deeper patches; Friedlaender et al. 2009, Ryan et al. 2013, Friedlaender et al. 2015). For each species, feeding whales were hypothesized to associate with higher total backscatter, higher intensity, lower dispersion, at shallower depths (based on optimal foraging theory, Doniol-Valcroze et al. 2011) than non-feeding whales.

4. Conditions targeted by feeding whales.—To constrain further the prey conditions that most influence feeding behavior, we used focal follow data and the same process as above to build binomial GAMs of the probability that a whale is feeding or not given local prey-related conditions. To allow interspecific comparison, the focus of this analysis was on euphausivory, so focal follows of humpbacks in which the predominant prey was fish were assigned behavior "Other." Beaufort belt density was replaced by a variable for tidal state (hours since the previous slack tide, calculated based on publicly available tidal predictions provided by the Canadian Hydrographic Service; Beauchemin Channel station). This was done because the interpolated dataset of BFT belt density was appropriate for spatial modeling, but lacks the time resolution to be relevant to feeding behavior.

5. Associated vs. available prey conditions.—Kolmogorov–Smirnov tests were used to compare the prey conditions associated with whales (sampled during focal follows) to those available within the fjord system within the same survey month (sampled during systematic transects). One-sided tests evaluated the hypotheses that whales, in all behavioral states, were found among backscatter with anomalously high total sum, high intensity, low dispersion, and shallow depth (after Doniol-Valcroze et al. 2011). In channels with double effort (see Fig. 2), only half of the transect data were used to build distributions of available conditions that represented the study area accurately.

A second, scale-sensitive approach compared associated conditions to available conditions at increasing distances from focal follows, the underlying premise being that positioning within the prey field is a central component to foraging strategy. To accomplish this, shortest path distances were calculated between each focal follow and the centroids of all 1-km transect bins from

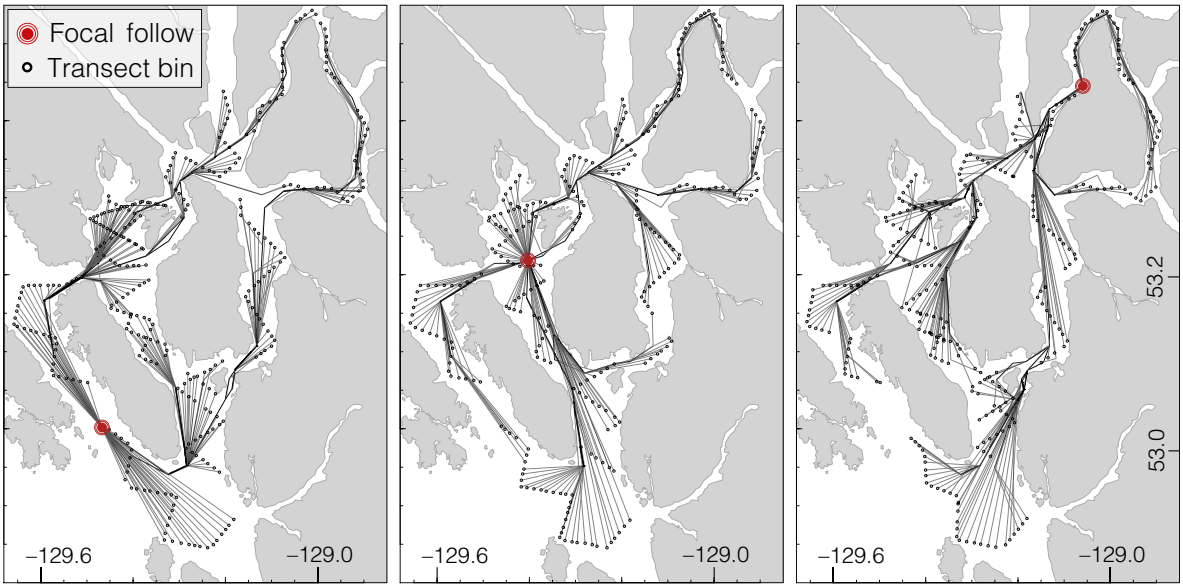

Fig. 5. Examples of "whale webs," the routine used to calculate shortest path distances (lines) between focal follows (red dot) and 1-km bins of echosounder data (black dots) collected during systematic transect surveys. Panels display examples of the routine for whales occurring in outer (left), central (center), and inner (right) channels of the Kitimat Fjord System.

the same survey month (examples in Fig. 5). Transect condition values were averaged such that each focal follow contributed no more than one datum regarding "available" conditions to each kilometer-wide bin from 0 km out to 80 km from the whale. Condition-distance datasets were then pooled from all focal follows for each species, and the mean and standard deviation of conditions within each kilometer bin were calculated. This process yielded a "position curve" depicting the mean position of whales with respect to available prey conditions within the fjord system. Position curves were calculated with raw data as well as with data scaled by median available conditions and best available conditions (95th quantile). Scaling was applied for each focal follow before pooling.

Position curve datasets were also used to test the spatial scale of context-dependent feeding behavior. The total 200 kHz backscatter in which whales were and were not feeding was modeled as a simple linear function of available conditions averaged at increasing radii from focal follows (2.5, 5, 10, and 20 km). The slope, regression coefficient, and *F*-statistic *P*-value of fit models were used to gauge the extent to which patterns in feeding decisions reflect patterns in nearby conditions.

Threshold functional response.—1. Aggregative thresholds.—To locate thresholds of aggregative response to total 200 kHz backscatter, I adapted the iterative step function analysis used by Piatt (1990) and Piatt and Methven (1992) for application within a likelihood framework. This allowed the same approach to be used for both aggregative and feeding threshold analyses (see proceeding 3 paragraphs).

A threshold response is a sigmoidal curve best modeled with a binomial regression with *logit* link function, which contains parameters that determine the inflection point of the curve (threshold, *T*), the maximum slope of the curve or growth rate (*R*), and the upper asymptote (*K*; Fig. 6):

$$f(x) = \frac{K}{1 + e^{-R(x-T)}}$$

Regression was performed in two stages. Stage 1 was to locate the threshold "height" (*T*, the prey value at the sigmoid's inflection point). I fit a binomial regression to 100 possible values spanning the range of sampled backscatter values (removing the 1st and 99th quantiles to

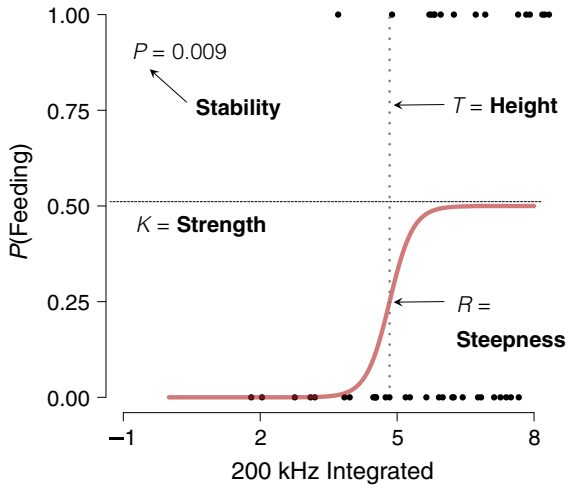

Fig. 6. Properties used to characterize threshold response to prey conditions. Variables *T*, *K*, and *R* correspond to parameters in the logistic regression. Threshold stability (*P*) is determined with Monte Carlo randomization (see *Methods*). Example data are behavioral modes (Feed = 1, Other = 0) from a focal follow on August 2015 as a function of total 200 kHz backscatter.

avoid boundary issues). During this fit, the sigmoid was forced into a step function (with *R* equal to the sample size of the dataset) such that *K* was the only parameter to be constrained using unweighted nonlinear least squares optimization in *R* (function "nls" in R). The "port" algorithm was used in order to create a lower bound of 0 for the growth rate. The test threshold whose regression returned the minimum AICc value was designated as the threshold.

In stage 2, the model was re-fit to the data allowing both *K* and *R* to be optimized. Their optimized values provided a measure of the "strength" and "steepness" of the threshold, respectively (Fig. 6). Higher values for *K* and *R* indicate a stronger and steeper threshold, respectively.

This process was first applied to unscaled data and then repeated for conditions when scaled by median and best (95th quantile) conditions available. Monte Carlo randomization (Manly 1991) was then used to ascertain the probability that threshold responses apparent in the data could have occurred by chance alone (sensu Piatt 1990). For 1000 iterations, observed whale densities were randomized with respect to prey observations and AICc of the best-fit model (parameterized using actual observations) was recalculated using the simulated data. The only constraint on randomized data was that the mean density above the threshold had to be greater than that below. The proportion of simulated AICc found to be lower than the observed AICc was interpreted as the probability that the location and shape of the observed response could be the result of random chance. This was taken as a measure of threshold "stability" (Fig. 6).

2. *Feeding thresholds.*—Feeding thresholds were located and tested using the same procedure as above for aggregative thresholds, but whale behavior rather than whale densities was treated as a function of prey-related variables. During model fitting, parameter constraints were used to ensure that regions of zero probability predicted by models did not conflict with non-zero data. Due to small sample size of fin whale focal follows (n = 33), only a single threshold was calculated for all years pooled.

3. *Context dependence of thresholds.*—To determine whether aggregative and feeding thresholds are a function of available conditions in general, humpback thresholds for each survey month were plotted against best available conditions. Low sample size (n = 6) precluded statistical analysis.

Results

Targeted prey conditions

Aggregative patterns.—Models of whale aggregation as functions of systematically sampled prey conditions are summarized in Table 3. I found overdispersion in whale count data, and the negative binomial model was selected over the Poisson and quasi-Poisson models based on visual inspection of quantile–quantile plots. For humpback whales, five of the 27 model fits were AICc-equivalent. These best-fit models included the variables seafloor depth, total backscatter (both frequencies), 200 kHz dispersion, and 200 kHz patch depth. Context-agnostic models explain humpback aggregation as fully as context-scaled models (AICc difference between rank 1 and 2 models, or ΔAICc = 2.9; r^2 of best fit = 0.42).

For fin whales, two of the 30 models fit were AICc-equivalent. These best-fit models included the variables seafloor depth, total backscatter (both

Table 3. Best-fit models of whale densities as a function of prey-related habitat features, based on transect data.

Model		Fit				Explanatory variables								
							200 kHz				33 kHz			
Species	*q*	*n* fit	*n* =	Min. AICc	r^2	Julian day	*T*	*I*	*D*	*Z*	*T*	*z*	bft	Debris
Humpback	Raw	27	5	698.3	0.42	*	***	. . .	*	*	**ns**	***	. . .	. . .
n = 159	50th	26	1	701.2	0.37	*	**	. . .	. . .	. . .	. . .	***	**ns**	. . .
	95th	26	8	704.4	0.34	**	***	ns	*	*	**	***	. . .	. . .
Fin	Raw	26	13	178.5	0.62	**ns**	ns	ns	**	ns	ns	*	ns	ns
n = 159	50th	21	7	176.6	0.60	**	ns	ns	***	ns	ns	***	. . .	ns
	95th	30	2	161.7	0.87	*	*	. . .	**	. . .	*	**	ns	. . .

Notes: Models were fit to three versions of the data (column *q*): raw data, data scaled by the median available conditions during the same survey month (50th quantile), and data scaled by the "best" available conditions (95th quantile). Model fit is described by number of variable combinations tested (*n* fit), the number of AICc-equivalent best-fit models (*n* =), the minimum AICc within that group (Min. AICc), and its r^2 (proportion of deviance explained by the model). Backscatter metric abbreviations follow those within Fig. 4. The variables included in best-fit models are denoted by their significance level (the highest found within best-fit set). ns, Not significant; AICc, corrected Akaike's information criterion.

Significance keys for spline functions of predictors: ns = $P > 0.05$; $^{*}P \leq 0.05$; $^{**}P \leq 0.01$; $^{***}P \leq 0.001$. Significance level symbols in boldface indicate variables included in model with minimum AICc. '. . .' refers to unavailable results.

frequencies), 200 kHz dispersion, and BFT belt density. Julian day was a significant variable for both species, reflecting seasonal changes in density. Fin whale aggregation is most explicable when using prey variables that are scaled by the best available conditions (95th quantile; ΔAICc = 15.1; $r^2 = 0.87$).

Spline functions provided insight into the relationships between prey variables and whale densities (Fig. 7). They indicate that humpbacks were more associated with moderate seafloor depths with high total 200 kHz backscatter that is relatively dispersed at an optimum depth of 95–115 m. Humpback distribution is governed more by krill-like backscatter than by fish-like backscatter, but at very high concentrations the 33 kHz backscatter gains some influence. According to models, humpbacks exhibit no significant relationships to the density of BFT belts or debris.

Spline functions indicate that fin whales were more associated with the deepest available waters with high total patches of 200 kHz backscatter that, contrary to what might be expected, is vertically dispersed. Also surprising is that total backscatter influences aggregative response only up to a relatively low value, beyond which the response curve flattens. Fins exhibit a negative relationship with areas of high densities of debris and tidal features.

Associated prey conditions.—Violin plots (Appendix S1: Fig. S1) and cumulative distribution functions (Appendix S1: Fig. S2) of the prey conditions sampled during focal follows revealed the importance of incorporating behavioral observations in prey preference studies, particularly when comparing two predator species. Strong differences in associated conditions between feeding and non-feeding whales were evident for some prey conditions (particularly total backscatter) but not all (e.g., debris density, 200 kHz intensity and dispersion). In general, feeding whales were found within a more restricted range of conditions than non-feeding whales. One-sided K–S tests corroborated these findings (Table 4). Below, *P* values above 0.95 are assumed to represent meaningful support for the alternate hypothesis of a one-sided test.

1. Interspecific differences.—Humpbacks of all behavioral states were found in a greater range of conditions than fin whales. Without behavioral resolution, the only significant preference differences between species were that humpbacks were found in higher 200 kHz intensity ($P = 0.997$) and fin whales were found among deeper patches ($P = 0.032$). For feeding whales, humpbacks were found in greater 200 kHz intensity ($P = 0.998$) and fins again were found among deeper patches ($P = 0.007$). Non-feeding humpbacks were also found among significantly higher 200 kHz intensity than non-feeding fins ($P = 0.962$), with no difference in patch depth ($P = 0.244$).

2. Intraspecific differences.—Feeding humpbacks were associated with higher backscatter total and

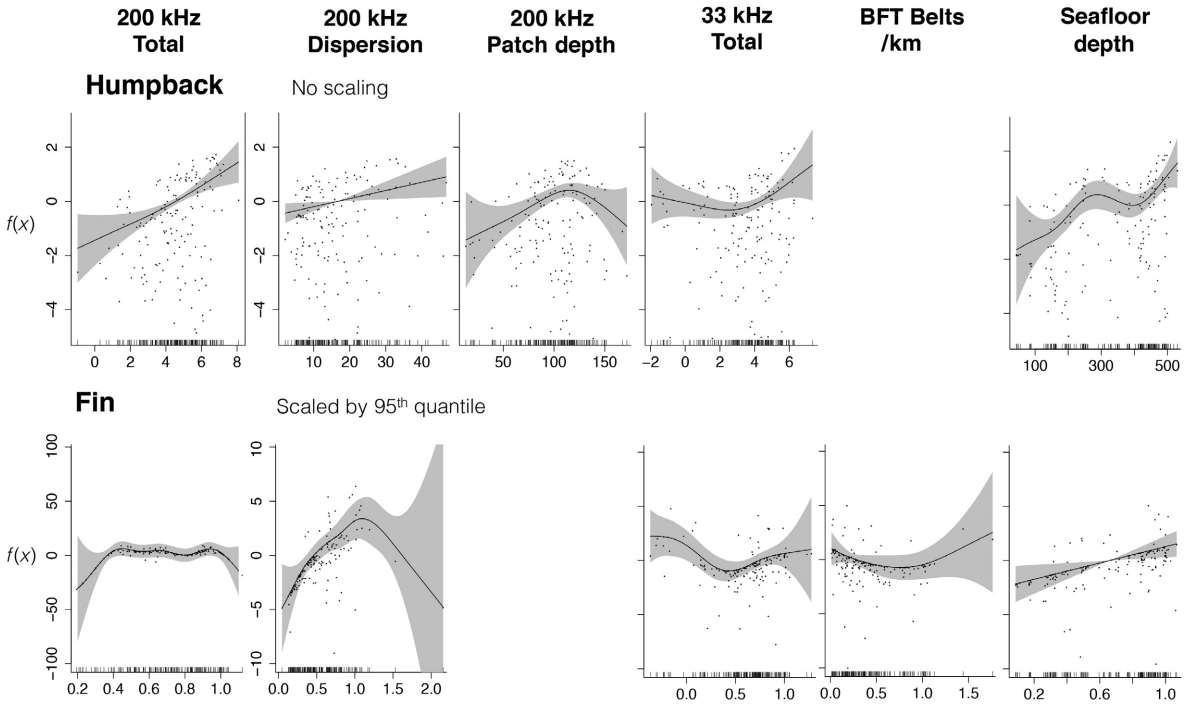

Fig. 7. Spline functions for best-fit models that predict whale densities based on prey-related habitat variables, both sampled during systematic transect survey effort. Humpback densities were best predicted by absolute measurements ("Abs," i.e. no scaling). Fin densities were best predicted when prey variables were scaled by "best" available conditions (95th quantile, $q = 0.95$). Gaps occur where variables were not included in any of the Akaike's information criterion-equivalent best-fit models. Plots feature superimposed residuals (dots) and ±1 SE bounds (gray shading). See Table 3 for detailed results.

intensity than non-feeding humpbacks ($P < 0.0001$ for both frequencies), but there was no difference in dispersion ($P = 0.387$) or patch depth ($P = 0.115$). Feeding fin whales were found in higher 200 kHz backscatter totals ($P < 0.001$) and lower dispersion ($P = 0.014$) than non-feeding fins, suggesting (contrary to aggregative GAM results) that fins were also targeting vertically compact prey layers.

3. 2015 monthly differences.—A large sample size in 2015 allowed humpback focal follows to be examined by survey month. Violin plots demonstrate that feeding humpbacks generally occurred in a more restricted range of conditions than non-feeding animals (Appendix S1: Fig. S3). Feeding whales were found in higher total backscatter with slightly higher intensity and slightly less dispersion. No strong inter-behavioral differences were evident for patch depth, seafloor depth, or debris densities. Throughout the summer, the discrepancy between behavioral states increased for total backscatter; non-feeding conditions declined, while feeding conditions remained consistent. Associated 200 kHz patch depth and dispersion increased throughout summer for both behavioral states. Whale distribution also became more dispersed and trended further inland (measured as distance from the fjord source; see Keen et al. 2017).

One-sided K–S tests were used to compare condition distributions month to month (Appendix S1: Table S1, Fig. S4). Feeding humpbacks were associated with significantly different total 200 kHz backscatter than non-feeders in all months except June 2015 ($P = 0.4483$; this was the month with highest overall total backscatter in the study area). Feeding whales targeted higher-intensity prey patches in most but not all months. In 2014, associated patch depth was shallower in feeding whales, but there was no difference

Table 4. Results of one-sided Kolmogorov–Smirnov tests for differences among prey conditions (mean ± SD reported for all) associated with whales (measured during focal follows) and available conditions within the study area (measured during systematic transects, first row of table).

			Backscatter metric				
			200 kHz				33 kHz
Species	Bhvr	*n*	Total	Intensity	Dispersion	Patch depth	Total
Study area		1739	3.36 ± 2.49	144.13 ± 17.87	10.89 ± 9.72	93.2 ± 38.44	2.33 ± 2.39
Humpback	All	350	4.85 ± 2.67	147.95 ± 20.21	10.50 ± 8.76	103.99 ± 31.83	0.49 ± 2.72
			$P_l < 0.000$	$P_l < 0.000$	$P_g = 0.125$	$P_g = 0.996$	$P_l = 0.844$
	Feed	136/40	6.43 ± 1.41	150.88 ± 19.46	10.46 ± 8.95	101.21 ± 31.57	5.73 ± 1.12
			$P_l < 0.000$	$P_l < 0.000$	$P_g = 0.113$	$P_g = 0.962$	$P_l < 0.000$
	Other	214/310	3.84 ± 2.8	145.76 ± 20.54	10.53 ± 8.64	106.22 ± 31.95	−0.18 ± 2.05
			$P_l < 0.001$	$P_l = 0.059$	$P_g = 0.456$	$P_g = 0.997$	$P_l = 1.000$
Fin	All	47	5.15 ± 2.11	140.92 ± 14.97	11.58 ± 6.87	116.25 ± 26.44	...
			$P_l < 0.000$	$P_l = 0.386$	$P_g = 0.699$	$P_g = 0.984$	
	Feed	27	6.13 ± 1.17	140.33 ± 14.73	9.76 ± 5.16	118.11 ± 23.9	...
			$P_l < 0.000$	$P_l = 0.229$	$P_g = 0.466$	$P_g = 0.972$	
	Other	20	3.78 ± 2.37	141.74 ± 15.63	14.27 ± 8.25	113.52 ± 30.26	...
			$P_l = 0.341$	$P_l = 0.928$	$P_g = 0.961$	$P_g = 0.993$	
Humpback	Feed vs. other		$P_l < 0.000$	$P_l < 0.000$	$P_g = 0.387$	$P_g = 0.115$	$P_l < 0.000$
Fin	Feed vs. other		$P_l < 0.00$	$P_l = 0.393$	$P_g = 0.014$	$P_g = 0.792$	...
Humpback vs. Fin	All		$P_g = 0.412$	$P_g = 0.997$	$P_l = 0.832$	$P_g = 0.032$	...
	Feed		$P_g = 0.940$	$P_g = 0.998$	$P_l = 0.679$	$P_g = 0.007$	...
	Other		$P_g = 0.441$	$P_g = 0.962$	$P_l = 0.945$	$P_g = 0.244$	...

Notes: Side of test is reported as subscript of *P* value; for "P_l," H_0 = case 1 < case 2; "P_g," H_0 = case 1 > case 2. Top section compares conditions found during various behavioral states to those available in study area; middle section compares conditions measured near feeding whales of same species to those near other behavioral states; bottom section compares conditions near humpbacks to those near fin whales. Column *n* reports the sample size used to calculate results (number of focal follows for each behavioral state, Bhvr; for study area, number of 1-km transect bins). When two sample sizes are reported, the first is for the total 200 kHz test and the second for total 33 kHz test. Sample size was too low for 33 kHz tests for fin whales.

between behavioral states in any month; dispersion was lower for feeding humpbacks in September 2015 only ($P = 0.0242$). Sample size for humpbacks feeding upon fish-like backscatter was too low for month-resolved analysis.

Conditions targeted by feeding whales.—Based on focal follow GAMs, prey conditions were better predictors of behavioral state for fin whales ($r^2 = 0.48$) than for humpbacks ($r^2 = 0.18$), and humpbacks appear to toggle feeding behavior according to a more complex suite of patch characteristics (Table 5). For humpbacks, 30 models were fit and four were AICc-equivalent. All variables but 200 kHz patch depth were included in one or more of these best-fit models, of which the following were significant at conventional levels: total 200 kHz ($P < 0.0001$), intensity ($P < 0.01$), seafloor depth, and tidal state ($P < 0.05$). For fin whales, 15 models were fit, of which eight were AICc-equivalent (discerning model fit was impaired by low sample size, $n = 45$). All variables were included in at least one best-fit model, but total 200 kHz was the only significant predictor ($P < 0.05$).

Associated vs. available prey conditions.—Histograms (Fig. 8) and cumulative distributions (Appendix S1: Figs. S2 and S4) reveal the ability of whales to locate anomalous prey conditions for certain variables, particularly for total backscatter metrics. One-sided K–S tests corroborate this and again demonstrate the importance of behavioral resolution in discerning prey preferences (Table 4; Appendix S1: Table S1). Ignoring behavioral state, humpbacks targeted areas with exceptionally high total 200 kHz backscatter ($P < 0.0001$) of high intensities ($P < 0.0001$) and great depth ($P = 0.996$). Fin whales targeted relatively high

Table 5. Best-fit generalized additive models of the probability that a whale is feeding among krill-like backscatter based on related habitat features sampled during focal follows 2014–2015.

Focal follows			Models				Explanatory variables: 200 kHz backscatter							
Species	*n*	*n* Fe	*n* fit	*n* =	Min. AICc	r^2	*T*	*I*	*D*	*Z*	*z*	Δ *z*	Tide	Debris
Humpback	277	135	30	4	332.7	0.18	***	**	**ns**	. . .	**	ns	*	ns
Fin	45	26	15	8	44.6	0.48	*	ns	ns	ns	ns	**ns**	ns	ns

Notes: *n*, total number of focal follows used in each species model; *n* Fe, number of *n* that were with feeding whales. Model fit is described by number of variable combinations tested (*n* fit), the number of AICc-equivalent best-fit models (*n* =), the minimum AICc within that group (Min. AICc), and its r^2 (proportion of deviance explained by model). Explanatory variables included in best-fit model set are denoted by their significance level (the highest found within best-fit models). Backscatter variable abbreviations follow those in Fig. 4. Other variables: *z* = mean seafloor within 1 km^2 of the geographic centroid of the focal follow; Δz = maximum slope within that same radius; tide = hours since the previous slack tide; debris = debris sightings per km surveyed. ns, Not significant; AICc, corrected Akaike's information criterion.

Significance key: ns = $P > 0.05$; $^{*}P \leq 0.05$; $^{**}P \leq 0.01$; $^{***}P \leq 0.001$. Significance levels in boldface indicate variables included in model with minimum AICc. An ellipsis (. . .) indicates variables not included in a best-fit model.

total backscatter ($P < 0.0001$) of great depth (both $P < 0.001$), but not of particularly high intensity ($P = 0.386$). Non-feeding humpbacks were found among higher total 200 kHz and patch depth ($P < 0.001$ and $P = 0.997$, respectively), but no differences were found between associated and available conditions for non-feeding fin whales. Feeding humpbacks were associated with significantly different conditions than those available for all variables except dispersion, while feeding fins were associated with higher total backscatter and greater patch depths only.

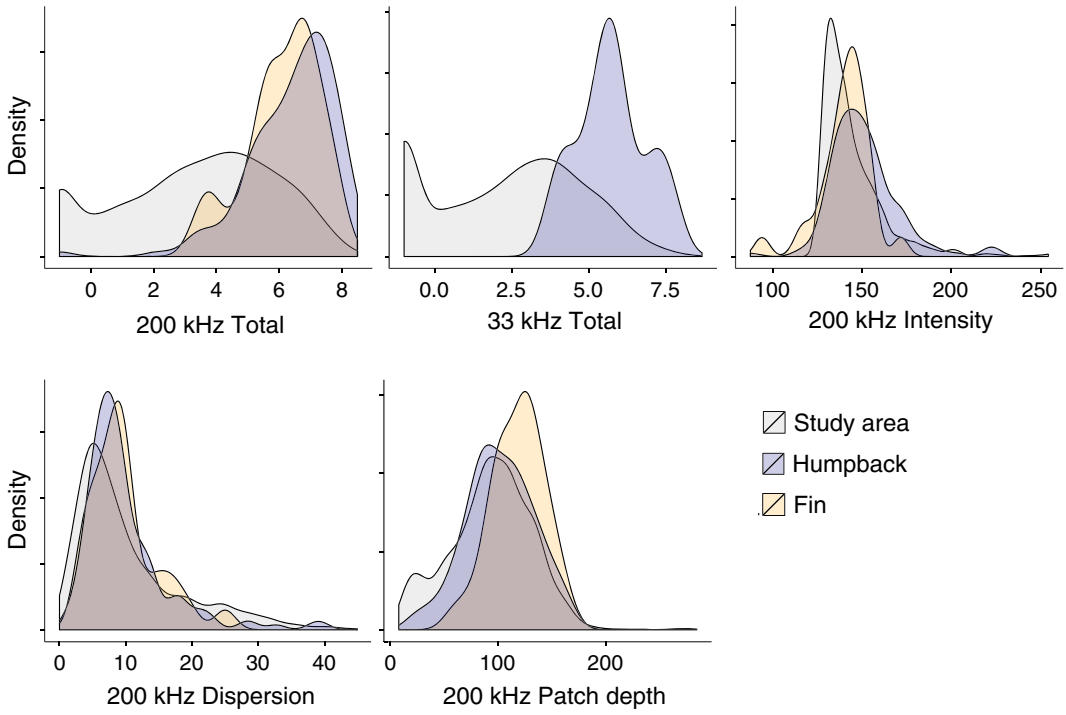

Fig. 8. Histograms of acoustic backscatter measured during focal follows of feeding whales. Distributions for fin whales (orange) and humpbacks (blue) can be compared to the distribution of "available conditions" (gray) sampled during systematic transect surveys. No feeding fin whales were found among non-zero 33 kHz backscatter levels.

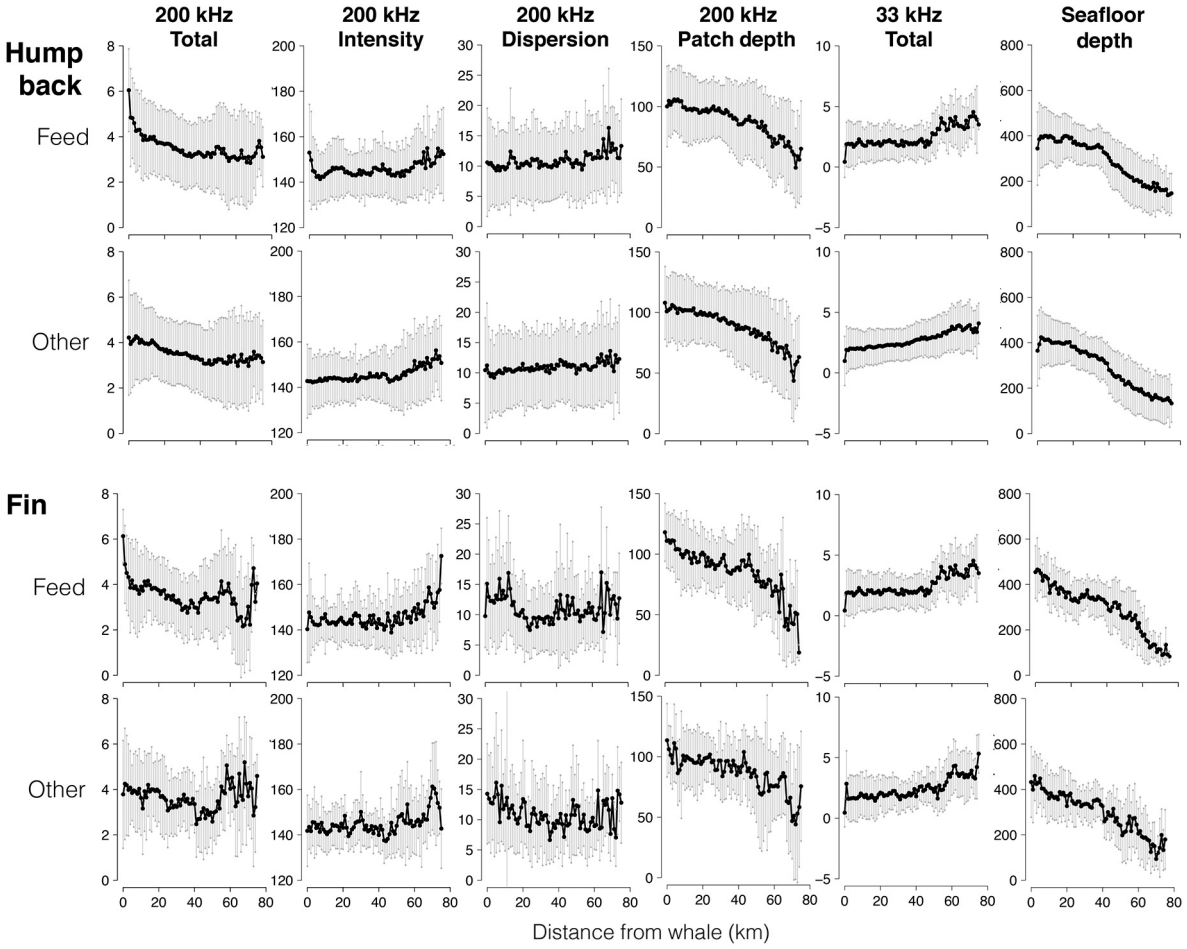

Fig. 9. Mean position of whales with respect to available prey-related habitat features (*columns*, sampled during systematic surveys), plotted according to distance (km) from the focal follow. "Position curves" for feeding and non-feeding ("Other") behavioral states are displayed for each species. Black line tracks the mean value within each 1-km distance window of all focal follows; vertical bars represent standard deviation.

Feeding humpbacks found anomalously intense 200 kHz backscatter in four of the six survey months (exceptions were August 2014 and September 2015). Associated dispersion was exceptional in September 2015 only ($P < 0.001$), and associated patch depth was exceptional only in August and September 2015 ($P = 0.977$ and 0.998, respectively). In 2015, feeding humpbacks found anomalously high total 200 kHz in all months ($P < 0.0001$ except June 2015, $P = 0.0036$).

Position curves.—Position curves provided insight into the effect size and spatial scale of whale–prey associations (Fig. 9). The most salient patterns were found for total 200 kHz, patch depth, and seafloor depth. Both humpback and fins, in both behavioral states, are positioned in the greatest 200 kHz patch depths available within the study area. There is no obvious pattern for 200 kHz dispersion or total 33 kHz curves, reinforcing the weak associations found in other analyses. The jaggedness of fin whale position curves is a product of low sample size.

Position curves also revealed that behavioral state is related to different spatial scales of association with prey (Fig. 9). Feeding whales were positioned in better conditions than non-feeding whales at both immediate scales and beyond. Curves were notably different between behavioral states for total 200 kHz backscatter for both species, 200 kHz patch depth for fin whales

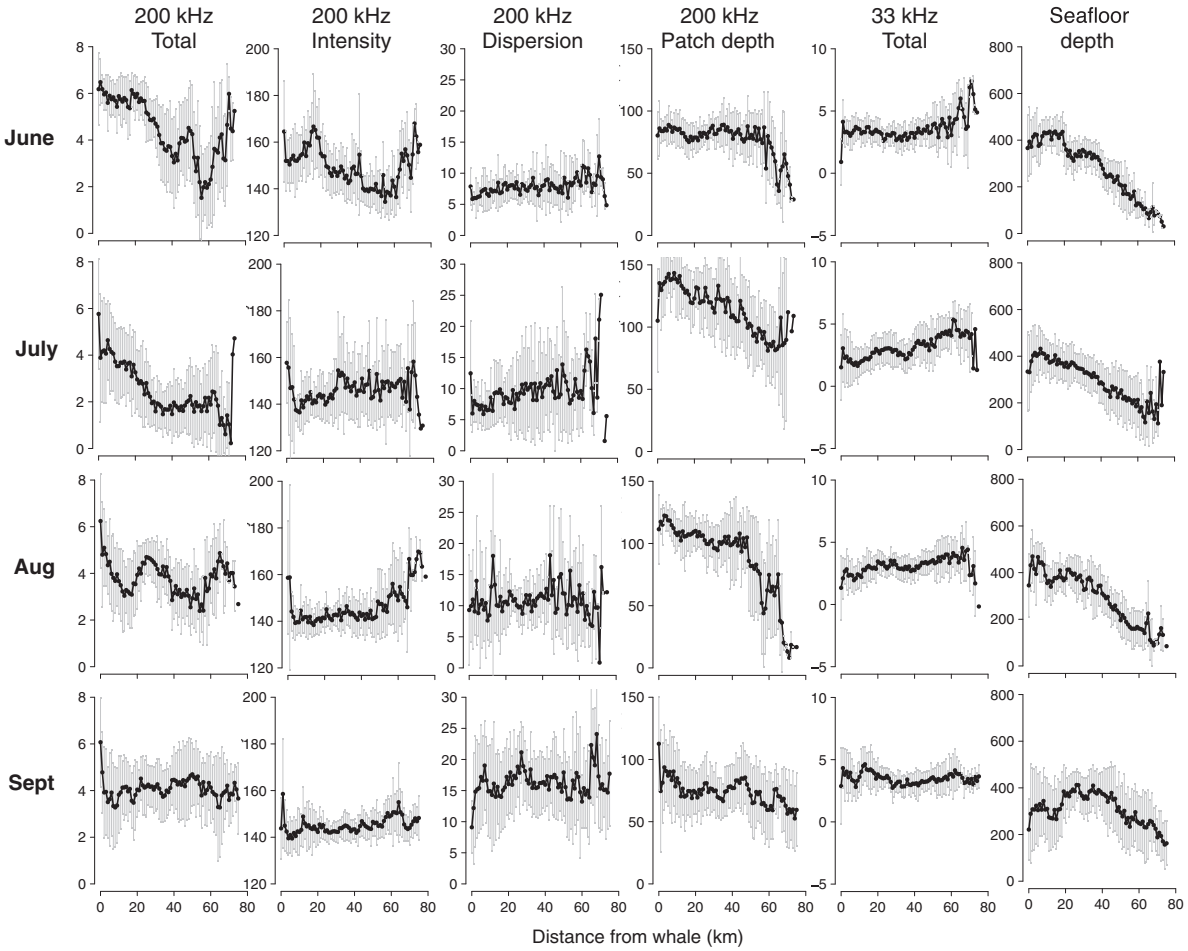

Fig. 10. Mean position of humpbacks with respect to available prey-related habitat features (columns, sampled during systematic surveys), plotted according to distance (km) from the focal follow, for each survey month of 2015 (rows). Black line tracks the mean value within each 1-km distance window of all focal follows; vertical bars represent standard deviation.

(feeding whales were positioned in the deepest patches available in the study area), and 200 kHz intensity for humpbacks (which spiked within 5 km of feeding whales). Feeding humpbacks, for example, remained on average among the highest total 200 kHz backscatter available within the study area; their position curve rises monotonically to the whale's mouths (km 0) from more than 30 km away. The non-feeding curve begins similarly, but levels off after only 15 km.

Position curves of 2015 humpbacks elucidate how dynamic spatial relationships between whales and prey-related habitat features can be from month to month (Fig. 10). Two notable findings are (1) that contrary to the 200 kHz patch depth curve in Fig. 9, patch depth is not maximized in every month and (2) that, for total 200 kHz, the spatial radius of condition optimization declines month to month; in the prey-rich month of June, humpbacks are at the summit of a broad, tall position curve that begins ascending monotonically 40 km away. By the prey-poor month of September, the monotonic increase begins only 5 km away, beyond which the position curve flat-lines. This pattern suggests that the spatial scale of whale–prey spatial association is a function of prey supply, and could explain instances of weak prey association found in studies using systematic survey methods (e.g., Logerwell and Hargreaves 1996, Keen et al. 2017).

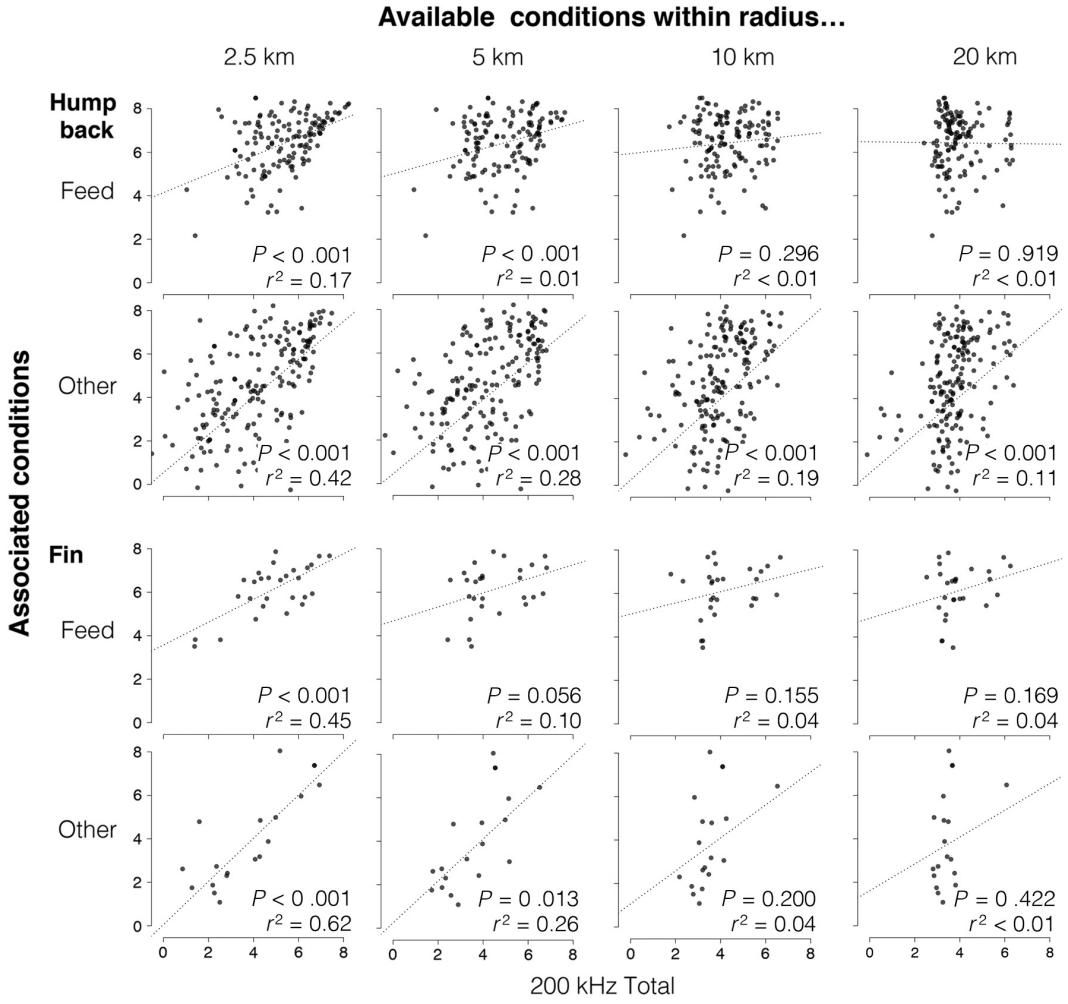

Fig. 11. Krill-like backscatter associations associated with whales as a function of the mean conditions available to them at increasing distances from the focal follow (columns; sampled during systematic transect surveys). Focal follows (dots) are separated by species and then by behavioral state (rows). For each scatterplot, fit of the linear regression (black line) is characterized by correlation coefficient (r^2) and P value of the F-statistic.

Scaled position curves (Appendix S1: Fig. S5) indicate that feeding humpbacks and fins are positioning themselves on average among total 200 kHz conditions that are nearly twice the median available in the study area. Conditions are above-median approximately 25 km out from humpbacks, but only 10 km out from fin whales. Their mean associated condition is just less than the 95th quantile of available conditions in the study area.

Spatial scale of context dependence.—As expected for both species, correlation between associated and available conditions decreased with increasing spatial scale used to measure available conditions (Fig. 11). Available conditions were strongly correlated with conditions associated with non-feeding whales out to moderate spatial scales (out to 20 km from the focal follow), but correlations with feeding conditions were weaker and more spatially confined. For humpbacks, feeding conditions were correlated with available conditions at radii 2.5 km ($P < 0.001$, $r^2 = 0.17$) and 5 km ($P < 0.001$, $r^2 = 0.01$), but not beyond. Non-feeding conditions were correlated with

Table 6. Summary of major findings.

		Available conditions			Associated conditions			Thresholds						
								Aggregative			Feeding			
Yr	Mo	50th	95th	Sp	Fe	Oth	Δ	*T*	*K*	*R*	*T*	*K*	*R*	$T_{FE} - T_{AG}$
All	All	3.64	7.02	H	6.43	3.84	2.59	3.28	0.39	20.0	4.78	0.72	0.85	1.50
				F	6.13	3.78	2.35	2.54	0.03	21.7	5.02	0.86	2.50	2.48
2014	All	3.29	6.75	H	6.47	4.20	2.27	5.08	1.04	1.3	5.05	0.63	2.0	−0.03
				F	…	…	…	3.28	0.05	245	…	…	…	
2015	All	3.84	7.13	H	6.40	3.65	2.75	3.16	0.35	16.5	4.77	0.75	0.7	1.61
				F	…	…	…	2.58	0.03	131	…	…	…	
Each survey														
2014	Aug	3.71	7.02	H	6.46	4.22	2.24	3.30	0.41	94.6	3.39	0.71	10.0	0.09
	Sep	2.88	6.51		6.50	4.16	2.34	5.06	0.73	311	4.94	0.65	2.5	−0.12
2015	Jun	5.29	7.83		6.41	5.96	0.45	5.28	0.30	232	4.69	0.86	0.1	−0.59
	Jul	1.85	6.87		6.49	3.86	2.63	6.17	1.43	3.0	6.17	1.00	0.4	0.00
	Aug	3.85	6.78		6.80	3.14	3.66	3.44	0.34	119	4.84	0.50	3.9	1.40
	Sep	4.28	6.56		6.39	2.13	4.26	1.91	0.66	2.7	3.5	0.78	78.4	1.59

Notes: Median and best available conditions are reported (50th and 95th quantiles, respectively, of total 200 kHz backscatter sampled during systematic transects) for various subsets of the 2014–2015 dataset (columns Yr, year, and Mo, month). Mean conditions associated with each species (Sp; H = humpbacks, F = fins) are reported for feeding whales (Fe) and those in some other behavioral state (Oth), followed by their difference (Δ). Threshold responses are characterized by height (*T*, in backscatter units), strength (*K*), and steepness (*R*) parameters for aggregative and feeding threshold types, and their difference ($T_{FE} - T_{AG}$). Fin whale summaries were only possible for the total combined dataset due to low sample size.

those available at all radii tested ($P < 0.001$ for all models). For fins, conditions amid feeding whales were correlated with available conditions only at radius 2.5 km ($P < 0.001$, $r^2 = 0.45$). Correlation for non-feeders was found out to 5 km only.

These differences signify that non-feeding conditions will reflect patterns of aggregation, while feeding conditions should only reflect the conditions in which it is energetically appropriate to feed. The spatially limited relationship found in feeding whales indicates that feeding decisions are in fact informed to some extent by nearby available conditions. This may explain the low predictive power of feeding GAMs, which did not account for local context. Interestingly, feeding focal follows appeared more strongly correlated with available conditions only when available conditions were high (see feeding humpbacks at radius 2.5 km, Fig. 11), implying that feeding decisions are context dependent only above a minimum threshold value.

Threshold functional response

Aggregative thresholds.—There was stronger evidence for threshold aggregative response in humpbacks than in fin whales (summary in Table 6; details in Appendix S1: Table S2; Fig. 12). Humpbacks also had a higher threshold than fins overall (3.28 vs. 2.54 total 200 kHz) and in each year (2014: 5.08 vs. 3.28; 2015: 3.16 vs. 2.58). For humpbacks, the aggregative threshold was placed at 75% of median available conditions and 53% of best available conditions (for fin whales, 59% and 42%, respectively).

Monte Carlo randomization indicated that the thresholds fit to fin whale aggregation were not significantly nonrandom ($P = 0.076$ for pooled dataset; Appendix S1: Table S2). Thresholds were much more stable for humpbacks in general ($P < 0.0001$ for pooled dataset), though evidence was weak in some months (August 2014, $P = 0.074$; September 2015, $P = 0.808$). In 2015, threshold height and stability generally decreased from month to month (Fig. 13). Thresholds found in raw data had higher stability than those regressed to context-scaled data.

Feeding thresholds.—For both species, there was strong evidence for feeding thresholds in response to increasing total 200 kHz backscatter (summary in Table 6; details in Appendix S1: Table S3; Fig. 14). Based on the entire dataset, the fin whale feeding threshold was higher than that of humpbacks (5.02 at $P < 0.001$ compared to 4.78 at $P < 0.001$), but humpbacks did have a higher threshold in July 2015 (6.17, $P = 0.078$).

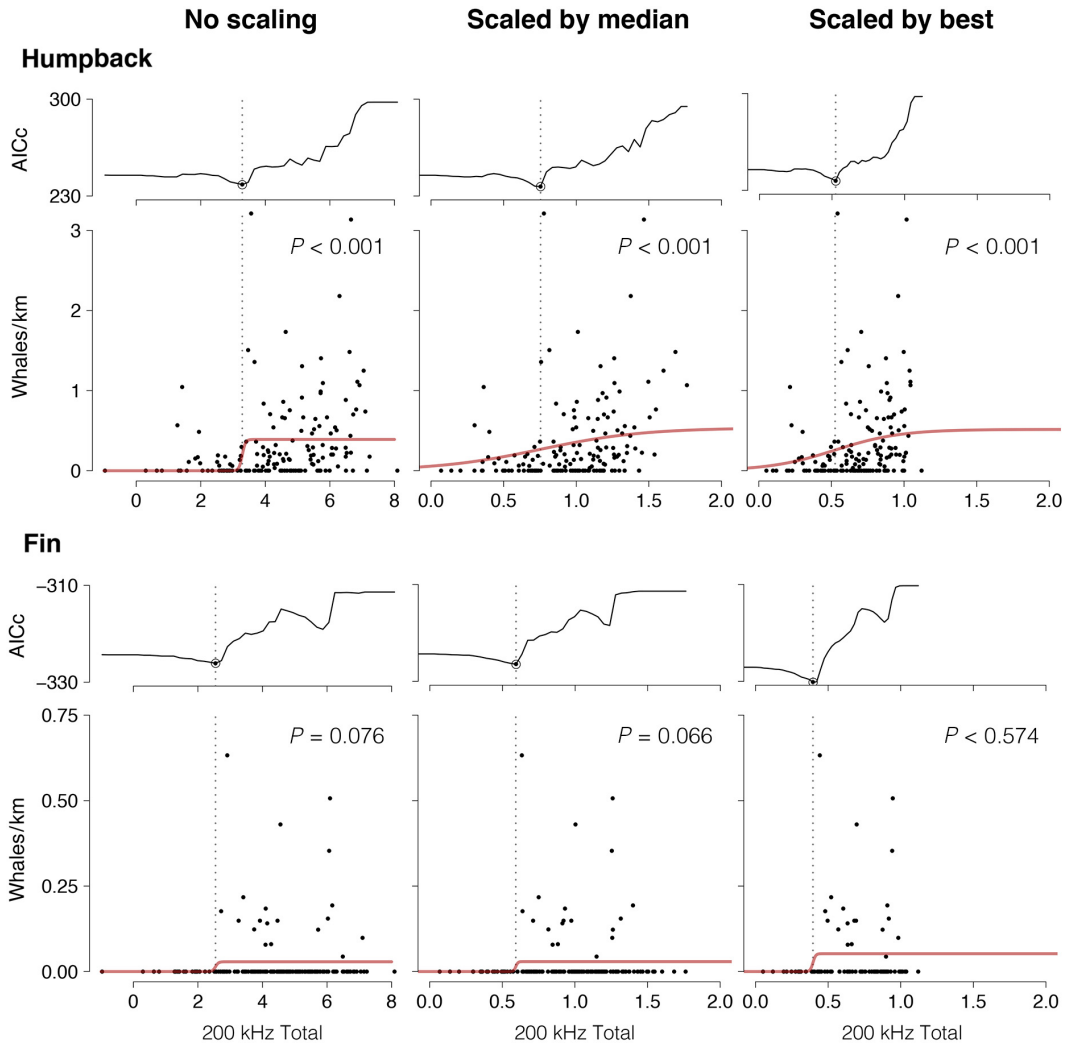

Fig. 12. Aggregative thresholds of humpback (top) and fin whale (bottom) response to changing totals of krill-like acoustic backscatter (*x*-axis, total 200 kHz). Models were fit to three versions of the data: raw (no scaling, left column), scaled by the median available conditions during the same year-month (50th quantile, center column), and scaled by the "best" available conditions (95th quantile, right column). Thresholds were located by iterative model fitting of sigmoidal regressions (red line) to prey conditions and associated whale densities (dots) sampled during systematic transect surveys. Line graphs atop each scatterplot display Akaike's information criterion (AICc) scores for each tested threshold; the value corresponding to the minimum AICc was deemed the threshold height. The *P* value of the threshold, displayed in each scatterplot, was determined with Monte Carlo randomization (see *Methods*).

Feeding threshold stability for humpbacks was low in June and July 2015 (Fig. 15), the 2 months with the highest best available conditions of the study. Throughout the 2015 summer, humpback feeding threshold stability and steepness increased, but threshold height was variable.

Context dependence.—To explore the context dependence of foraging strategy overall, available conditions in each survey month were plotted against mean associated conditions and threshold heights (Table 6, Fig. 16). With only six surveys to compare, statistical tests were not

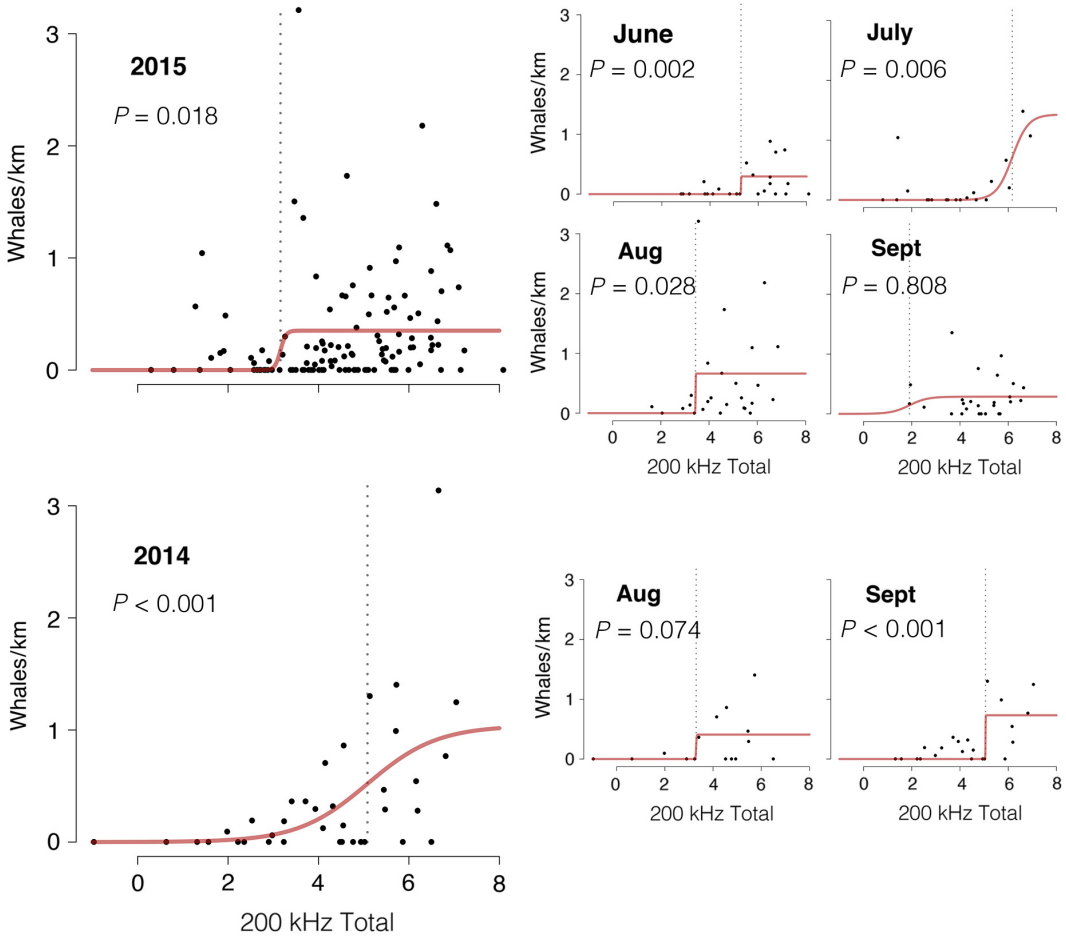

Fig. 13. Aggregative thresholds of humpback response to changing totals of krill-like acoustic backscatter (*x*-axis, total 200 kHz) for each year (left column, larger panes) and then for each survey month within year (smaller panes on right). Thresholds were located by iterative model fitting of sigmoidal regressions (red line) to prey conditions and associated whale densities (dots) sampled during systematic transect surveys. The *P* value of the threshold, displayed in each scatterplot, was determined with Monte Carlo randomization (see *Methods*).

possible. Mean conditions associated with feeding whales do not appear related to available conditions (Fig. 16A), but those associated with non-feeding humpback whales do (Fig. 16B), causing their ratio (the "feeding ratio") to decrease with increasing available conditions (Fig. 16C). Similarly, feeding thresholds do not appear related to available conditions (Fig. 16D), but aggregation thresholds do (Fig. 16E), causing their ratio (the "threshold ratio") to decrease with increasing available conditions (Fig. 16F).

Intriguing patterns in these relationships were also found in 2015 humpback data (Fig. 17). Best available conditions declined throughout the summer (Fig. 17A); this decline is reflected in the mean conditions sampled when with non-feeding whales (Fig. 17B). However, the mean conditions in which whales were feeding remained constant (Fig. 17C), causing the feeding ratio to increase throughout summer (Fig. 17D). Aggregation and feeding thresholds followed similar trajectories, peaking in July and then declining through September (Fig. 17E, F). This pattern was less dramatic in feeding thresholds, causing the threshold ratio to increase throughout the summer as well (Fig. 17G). As best available conditions and the height of aggregation thresholds declined, so too did aggregation threshold

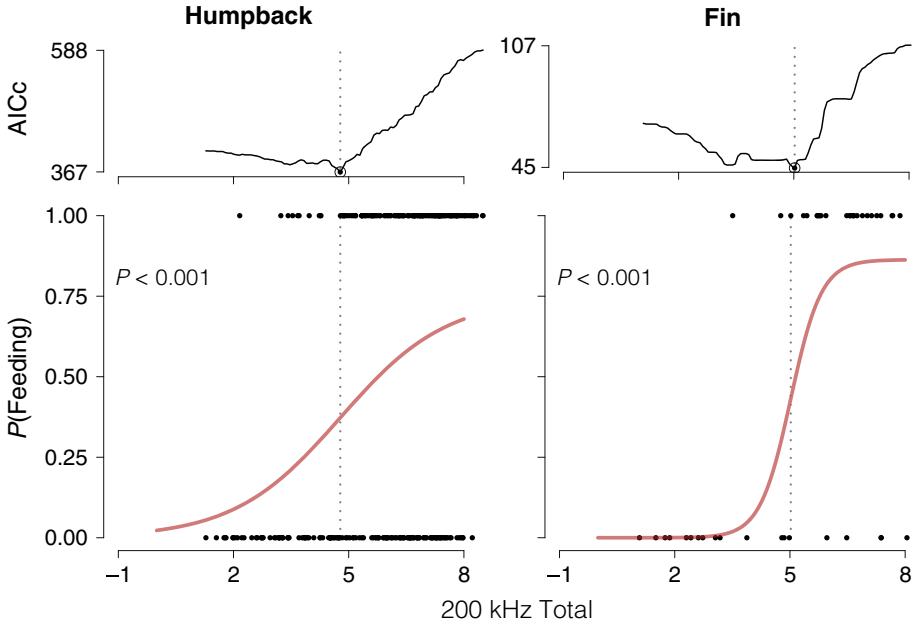

Fig. 14. Feeding thresholds of humpback (left) and fin whale (right) in response to changing totals of krill-like acoustic backscatter (*x*-axis), located by fitting logistic regressions (red line) that model the probability of a whale (dots) feeding ($y = 1$) or not ($y = 0$) given backscatter present. Regressions were fit to each backscatter value within the dataset range; the value whose regression yielded the minimum Akaike's information criterion (AICc) value was designated as the threshold (line graph atop each scatterplot displays AICc scores for tested thresholds). The *P* value of the threshold, displayed in each scatterplot, was determined with Monte Carlo randomization (see *Methods*).

stability (reflected in the increasing *P*-value of Monte Carlo randomization test; Fig. 17H). Conversely, feeding threshold stability and steepness increased (Fig. 17I, J).

Discussion

Within the context of a complex coastal habitat, in which multiple prey-related habitat features were found to influence whale aggregation and feeding effort, I observed both aggregative and feeding threshold responses to increasing krill supply in two species of rorqual: humpback and fin whales. Overall, findings align with the expectations that aggregative behavior is responsive to local context, while feeding thresholds are governed by the less mutable energetic constraints imposed by feeding mode. As a result, the height difference of the two thresholds appears to be context dependent, as would be the expected ecological implications of their difference (see *Introduction*). For both threshold types in humpbacks, threshold stability appeared to be a function of local conditions: As total krill-like backscatter increased, aggregative thresholds stabilized and feeding thresholds destabilized (Fig. 17). In prey-poor areas, aggregative response seems to degrade to another response type or even into no response at all, while feeding response steepens and stabilizes.

This study explored whale–prey associations from three vantages: systematic distribution surveys, behavioral focal follows, and "position curves," a novel technique that fuses the first two. While all vantages seem indispensable, I cannot overstate the importance of behavioral observations alongside prey sampling in my objective of identifying the prey-related habitat features that each species is targeting. Results of spatial association modeling based upon systematic surveys were incomplete and, in some cases, misleading. Position curves were particularly useful in explaining the discrepancies between systematic and focal follow findings. For example, position

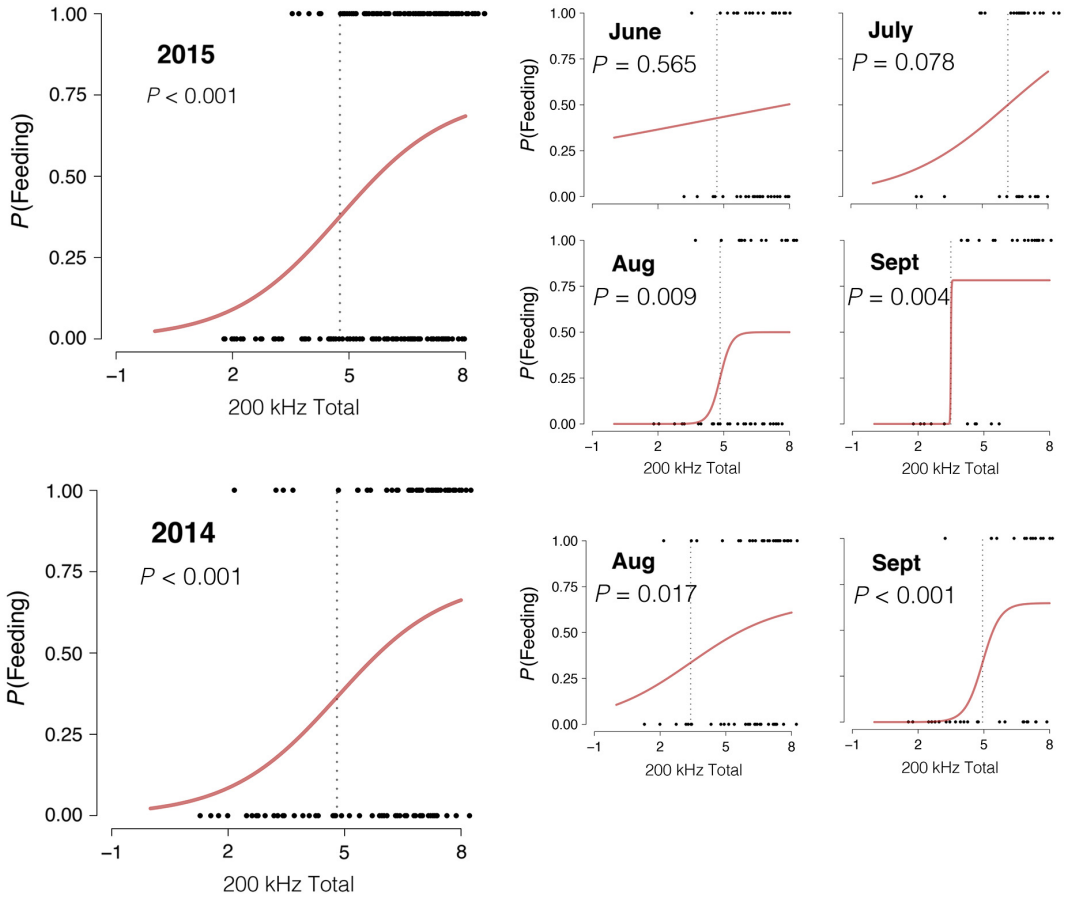

Fig. 15. Feeding thresholds of humpback whales in response to changing totals of krill-like acoustic backscatter (x-axis), located by fitting logistic regressions (red line) that model the probability of a whale (dots) feeding ($y = 1$) or not ($y = 0$) given backscatter present. Thresholds were found for each year of data (left column, larger panes) and then for each survey month within year (smaller panes on right). The P value of the threshold, displayed in each scatterplot, was determined with Monte Carlo randomization (see *Methods*).

curves showed that fin whales feed in broad areas of high dispersion, but dispersion appeared to decline within 5 km of the fin whales sampled (Fig. 9). This may explain the discrepancy between their aggregative relationship with high dispersion (Fig. 7) and their feeding relationship with low dispersion (Table 4).

From all vantages, humpback association with and behavioral response to prey-related habitat features were less predictable and affected by more factors than that of the fin whale, which appeared to be exclusively euphausivorous and interested predominantly in the total amount and depth of krill-like backscatter within the deepest channels. Humpbacks used more of the study area (Fig. 3), fed in a wider range of conditions (Appendix S1: Fig. S1), fed upon both euphausiids and small schooling fish (Fig. 8), toggled feeding effort according to a more complex suite of patch characteristics (Table 5), positioned themselves more consistently within the best feeding conditions available within the entire study area (Figs. 9 and 10), adjusted aggregation and feeding decisions based on a larger context radius (Fig. 11), found larger prey patches (in both feeding and non-feeding behavioral states, Table 6), and exhibited higher aggregative thresholds (Table 6). And yet, despite all this evidence that humpbacks are "better" foragers within the KFS than fin whales, the feeding threshold for fin whales was higher than that of humpbacks (Table 6). These findings, which are in alignment with the expectations of

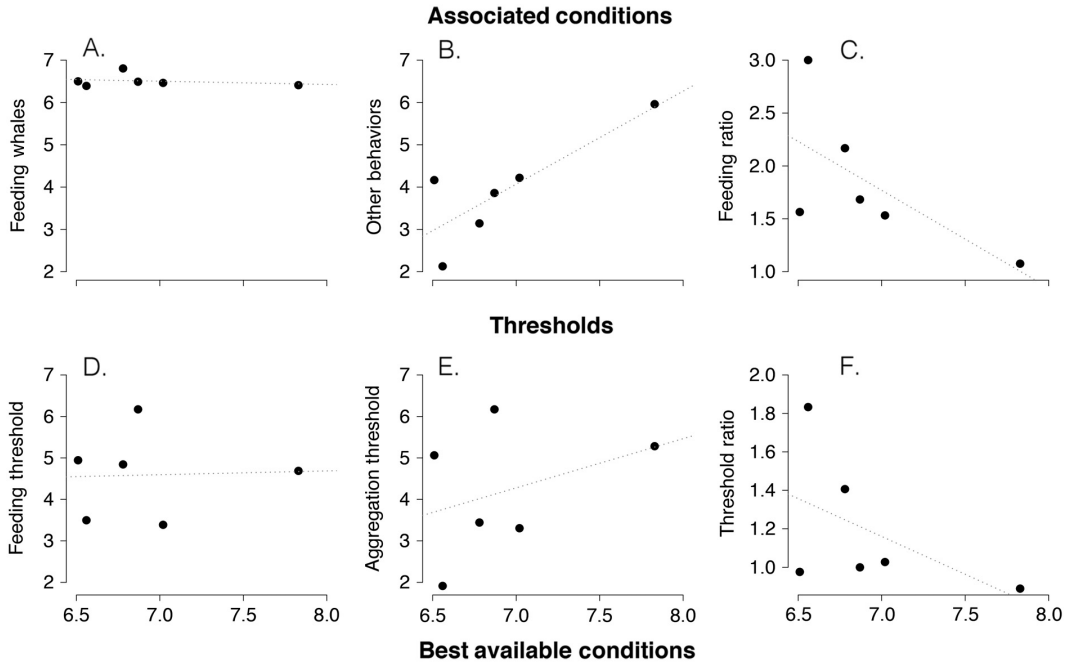

Fig. 16. Summary of humpback response to changes in the best available krill-like conditions (the 95th quantile of total 200 kHz backscatter sampled during systematic surveys, *x*-axes). Each dot represents a survey month ($n = 6$, two from 2014 and four from 2015). (A) Mean conditions associated with feeding whales do not appear related to available conditions, but (B) those associated with non-feeding whales do, causing (C) their ratio (the "feeding ratio") to decrease with increasing available conditions. (D) Feeding thresholds do not appear related to available conditions, but (E) aggregation thresholds do, causing (F) their ratio (the "threshold ratio") to decrease with increasing available conditions. Far right dot is June 2015. Superimposed lines are simple linear models fit to the six data.

energetics (Goldbogen et al. 2007, 2008), further support the energetic, context-independent basis for feeding threshold height. They also suggest that aggregative thresholds can be a function not only of energetic requirements, but also of foraging strategy and habitat familiarity. While humpbacks may benefit from prey patches within this fjord system that far surpass their feeding threshold, they also benefit from being able to feed profitably at lower prey densities than a larger close relative.

The finding that feeding thresholds were generally higher than aggregative thresholds is the opposite of that in the only other whale-focused study that has compared the two threshold types, Feyrer and Duffus (2015). Their disagreement may reflect the energetic differences between gray whale feeding upon benthic and epibenthic prey, in their study, and the rorqual lunge feeding studied here.

That humpbacks were better positioned within prey-rich regions alongside prey-like backscatter that had higher totals, higher intensity, and lower vertical dispersion than were fin whales, begs the question of how. It seems key that humpbacks are willing to explore the entirety of the fjord system, rather than just a few of its channels as fin whales do. Beyond that, however, I hypothesize (1) that humpbacks are more attuned and responsive than fin whales are to oceanographic indicators of foraging opportunities within the fjord system (as suggested by the importance of tidal state in humpback behavioral state, Table 4), (2) that humpbacks maintain their intimacy with prey and environmental cues via more thorough strategies of travel and exploratory diving, (3) that the much higher density of humpbacks within the fjord system increases the chances of encountering better prey patches, to which other humpbacks can then be alerted via

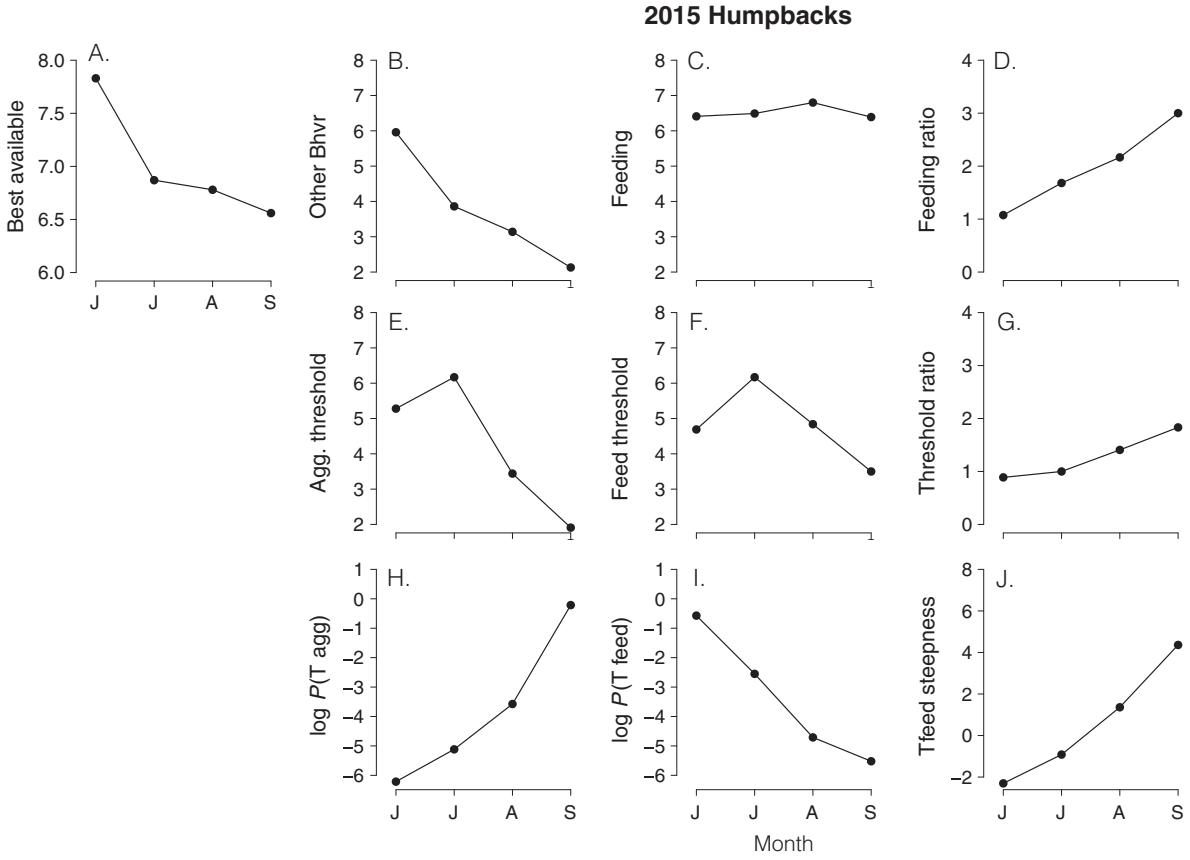

Fig. 17. Month-to-month patterns in the relationship between humpbacks and krill-like prey conditions (total 200 kHz backscatter) in 2015 (June, July, August, and September). (A) The best available conditions (95% quantile of backscatter sampled on systematic transects) decline throughout the summer. (B) Humpbacks in non-feeding behavioral states are found in declining prey conditions. (C) Feeding humpbacks maintain consistent prey conditions throughout the season, causing (D) the ratio between feeding and non-feeding conditions to increase. (E) Aggregative thresholds peak and then decline, as do (F) feeding thresholds though more slowly, causing their ratio (G) to increase similar to the feeding ratio. (H) The *P* value of the aggregative threshold (determined by Monte Carlo randomization) increases throughout the summer, but (I) that of the feeding threshold declines. (J) The steepness (growth parameter *R*) of feeding thresholds increases throughout the summer.

some acoustic, visual, or otherwise social cue, and (4) that the euphausivorous fish targeted by humpbacks when not feeding upon krill serve to maintain and perhaps even enhance humpback-krill spatial association (J. Pilkington, *personal communication*). Hypotheses 1 and 2 are testable with data from the same fieldwork conducted for this study, and these analyses are forthcoming.

The most curious finding revealed by focal follow sampling and position curve analysis was that whales were positioning themselves amid the deepest prey patches available (Fig. 9), which seems to go against current paradigms of optimal foraging theory for rorqual whales (Doniol-Valcroze et al. 2011). This was true for both species, but the pattern was particularly strong for fin whales. Dive-ventilation metrics, collected during the fieldwork for this study, may offer insight into the foraging effort strategies employed by each species within various prey contexts. These analyses are also forthcoming.

Laidre et al. (2010) found a similar preference for deeper krill patches in Greenland whales, but they suspected that it was due to the low krill volume typical of shallow shelf waters. This is not a viable explanation in the present study.

Friedlaender et al. (2015) found that a blue whale feed deeper for longer dives than a sympatric fin whale, proposing that competition may have compelled the two species to partition the prey field. Prey or habitat partitioning has been offered as explanations of prey preference differences in other studies (Friedlaender et al. 2009, Ryan et al. 2013), which have noted the potential implications for ecosystem diversity and stability. Humpbacks and fins in the present study system can be said to be competing for the same prey resource, and certain of their prey-related habitat preferences do differ. However, to the extent that "partitioning" also implies a *response* of predators to their co-occurrence, the findings presented here are compatible with but not suggestive of it. An alternative hypothesis is that euphausiids within the fjord systems are vertically structured by taxon or demography and thus by nutrient content (Decima et al. 2010), which may differentially suit the capture abilities and/or energetic needs of humpbacks and fins.

Fin whales seem to prefer only a few waterways within the KFS, but are consistently positioned among the deepest krill-like backscatter in the deepest waters, and this backscatter is consistently among the highest total available in any given summer month. These facts may reflect underlying mechanisms, likely oceanographic in nature, that render these fjord channels specifically suitable for fin whales. This in turn may explain the historical importance of this fjord system to fin whales relative to apparently similar systems to the north and south which fin whales rarely use (Nichol and Ford 2011, Ford 2014), and invites particular caution in the assessment of proposed industrial developments within this fjord system.

Like all spatial patterns, that of predator–prey interactions may only be strong, stable, and/or apparent at certain scales (Levin 1992). While overlap with prey must occur on the smallest scale in order for feeding to occur, predators must seek out and position themselves for that opportunity by navigating and assessing prey conditions at multiple nested spatial scales. Position curve analysis proved a particularly enriching means of exploring the spatial scale of interactions between whales and prey-related habitat features, and there is much room for further refinement and application of this tool. Care should be taken with its application, however, as its value is contingent upon the appropriate balance of scales in survey design; spatial coverage must sufficiently comprehend available habitat and temporal coverage must be sufficiently synoptic. The multiple perspectives used in this study, and the emergent insight they yielded, were made possible by the dual design of systematic surveys punctuated by focal follows, with oceanographic sampling during both research modes. Further implementation of this dual design in coastal systems would be of great value as we strive to understand, appreciate, and restore the role of large pelagic predators in marine systems.

Acknowledgments

Bangarang fieldwork was conducted under federal permit (DFO XR 83 2014) in collaboration with North Coast Cetacean Society and formal research agreement with the Gitga'at First Nation. *Bangarang* fieldwork was funded by the Gitga'at First Nation Guardian Watchmen, Canadian Department of Fisheries and Oceans, Cascadia Research Collective, NSF Graduate Research Fellowship program (DGE-114086), Lewis and Clark Fund, National Geographic Society - Waitt Grant (2681-13), and private donations from the Watson, Ayres, Cunningham, Barlow, and Keen families. Katie Qualls provided preliminary analyses on euphausiid data. This work would also not be possible without the direction and mentorship of Hermann Meuter, Janie Wray, or Chris Picard, nor without the dedication, skills, and friendship of *Bangarang* crew: Will and Keri Watson, Katie Qualls, Dylan and Luke Padgett, Richard Candler, Matt Irwin, Nelle Pierson, Kelly Beach, Jonathan Carpenter, Mike Keen, Kim-Ly Thompson, Will Bostwick, Jay Barlow, Barb Taylor, Anne Simonis, Sam Watson, Emily Ezell, Sara Keen, Nicholas Bruns, and Jeff Garretson.

Literature Cited

Abrams, P. 1983. The theory of limiting similarity. Annual Review of Ecology and Systematics 14:359–376.

Akaike, H. 1974. A new look at the statistical model identification. IEEE Transactions of Automatic Control 19:716–723.

Alexander, R. M. 2005. Models and the scaling of energy costs for locomotion. Journal of Experimental Biology 208:1645–1652.

Ashe, E., J. Wray, C. R. Picard, and R. Williams. 2013. Abundance and survival of Pacific humpback whales in a proposed critical habitat area. PLoS ONE 8:e75228.

Barlow, J., et al. 2011. Humpback whale abundance in the North Pacific estimated by photographic capture-recapture with bias correction from simulation studies. Marine Mammal Science 27:793–818. https://doi.org/10.1111/j.1748-7692.2010.004444.x

Berta, A., J. L. Sumich, and K. M. Kovacs, editors. 2006. Marine mammals: evolutionary biology. Second edition. Academic Press, Burlington, Massachusetts, USA.

Buckland, S. T., D. R. Anderson, K. P. Durham, J. L. Laake, D. L. Borchers, and L. Thomas. 2001. Introduction to distance sampling: estimating abundance of biological populations. Chapman and Hill, New York, New York, USA.

Burnham, K. P., and D. R. Anderson. 2002. Model selection and multimodel inference: a practical information-theoretic approach. Second edition. Springer-Verlag, New York, New York, USA.

Chakravarti, L., and J. Roy. 1967. Handbook of methods of applied statistics. Volume 1. John Wiley and Sons, Hoboken, New Jersey, USA.

Chenoweth, E. M., C. M. Gabriele, and D. F. Hill. 2011. Tidal influences on humpback whale habitat selection near headlands. Marine Ecology Progress Series 423:279–389.

COSEWIC. 2005. COSEWIC assessment and update status report on the fin whale, Balaenoptera physalus, in Canada. Committee on the Status of Endangered Wildlife in Canada, Ottawa, Ontario, Canada.

Croll, D. A., A. Acevedo-Gutierrez, B. R. Tershy, and J. Urban-Ramirez. 2001. The diving behavior of blue and fin whales: Is dive duration shorter than expected based on oxygen stores? Comparative Biochemistry and Physiology Part A: Molecular & Integrative Physiology 129:797–809.

Croll, D. A., B. Marinovic, S. Benson, F. P. Chavez, N. Black, R. Ternullo, and B. R. Tershy. 2005. From wind to whales: trophic links in a coastal upwelling system. Marine Ecology Progress Series 289:117–130.

De Leeuw, J. J. 1999. Food intake rates and habitat segregation of tufted duck, *Aythya fuligula,* and scaup, *Aythya marila,* exploiting zebra mussels, *Dreissena polymorpha*. Ardea 87:15–31.

Decima, M., M. D. Ohman, and A. de Robertis. 2010. Body size dependence of euphausiid spatial patchiness. Limnology and Oceanography 55:777–788.

Dolphin, W. F. 1987. Ventilation and dive patterns of humpback whales, *Megaptera novaeangliae*, on their Alaskan feeding grounds. Canadian Journal of Zoology 65:83–90.

Doniol-Valcroze, T., V. Lesage, J. Giard, and R. Michaud. 2011. Optimal foraging theory predicts diving and feeding strategies of the largest marine predator. Behavioral Ecology 22:880–888.

Feyrer, L. J., and D. A. Duffus. 2015. Threshold foraging by gray whales in response to fine scale variations in mysid density. Marine Mammal Science 31:560–578.

Flinn, R. D., A. W. Trites, E. J. Gregr, and R. I. Perry. 2002. Diets of fin, sei, and sperm whales in British Columbia: an analysis of commercial whaling records, 1963–1967. Marine Mammal Science 18: 663–679.

FOC [Fisheries and Oceans Canada]. 2013. Recovery strategy for the North Pacific Humpback Whale (Megaptera novaeangliae) in Canada. Species at Risk Act Recovery Strategy Series. Fisheries and Oceans Canada, Ottawa, Ontario, Canada.

Forcardi, S., P. Marcellini, and P. Montanaro. 1996. Do ungulates exhibit a food density threshold? A field study of optimal foraging and movement patterns. Journal of Animal Ecology 65:606–620.

Ford, J. K. B. 2014. Marine mammals of British Columbia. First edition. Royal BC Museum, Victoria, British Columbia, Canada.

Friedlaender, A. S., J. A. Goldbogen, E. L. Hazen, J. Calambokidis, and B. L. Southall. 2015. Feeding performance by sympatric blue and fin whales exploiting a common prey resource. Marine Mammal Science 31:345–354.

Friedlaender, A. S., P. N. Halpin, S. S. Qian, G. L. Laweson, P. H. Wiebe, D. Thiele, and A. J. Read. 2006. Whale distribution in relation to prey abundance and oceanographic processes in shelf waters of the Western Antarctic Peninsula. Marine Ecology Progress Series 317:297–310.

Friedlaender, A. S., G. L. Lawson, and P. N. Halpin. 2009. Evidence of resource partitioning between humpback and minke whales around the western Antarctic Peninsula. Marine Mammal Science 25:402–415.

Goldbogen, J. A., D. Cade, J. Calambokidis, A. S. Friedlaender, J. Potvin, P. S. Segre, and A. Werth. 2017. How baleen whales feed: the biomechanics of engulfment and filtration. Annual Review of Marine Science 9:367–386.

Goldbogen, J. A., J. Calambokidis, D. Croll, J. Harvey, K. Newton, E. Oleson, G. Schorr, and R. E. Shadwick. 2008. Foraging behavior of humpback whales: Kinematic and respiratory patterns suggest a high cost for a lunge. Journal of Experimental Biology 211:3712–3719.

Goldbogen, J. A., J. Calambokidis, E. Oleson, J. Potvin, N. D. Pyenson, G. Schorr, and R. E. Shadwick. 2011. Mechanics, hydrodynamics, and energetics of blue whale lunge feeding: efficiency dependence on krill density. Journal of Experimental Biology 214:131–146.

Goldbogen, J. A., N. D. Pyenson, and R. E. Shadwick. 2007. Big gulps require high drag for fin whale lunge feeding. Marine Ecology Progress Series 349:289–301.

Gregr, E. J., J. Calambokidis, L. Convey, J. K. B. Ford, R. I. Perry, L. Spaven, and M. Zacharias. 2006. Recovery strategy for blue, fin, and sei whales (*Balaenoptera musculus*, *B. physalus*, and *B. borealis*) in Pacific Canadian waters. Species at Risk Act Recovery Strategy Series. Fisheries and Oceans Canada, Vancouver, British Columbia, Canada.

Hamilton, P. K., G. S. Stone, and S. M. Martin. 1997. Note on a deep humpback whale, *Megaptera novaeangliae* dive near Bermuda. Bulletin of Marine Science 61:491–494.

Hassell, M. P., and R. M. May. 1974. Aggregation of predators and insect parasites and its effect on stability. Journal of Animal Ecology 43:567–594.

Hastie, T. J., R. Tibshirani, and J. Friedman. 2009. The elements of statistical learning: data mining, inference and prediction. Second edition. Springer-Verlag, New York, New York, USA.

Hilbe, J. M. 2011. Negative binomial regression. Second edition. Cambridge University Press, New York, New York, USA.

Hines, A. H., R. B. Whitlatch, S. F. Thrush, J. E. Hewitt, V. J. Cummings, P. K. Dayton, and P. Legendre. 1997. Nonlinear foraging response of a large marine predator to benthic prey: eagle ray pits and bivalves in a New Zealand sand flat. Journal of Experimental Marine Biology and Ecology 216:191–210.

Hollings, C. S. 1965. The functional response of predators to prey density and its role in mimicry and population regulation. Memoirs of the Entomological Society of Canada 45:1–60.

Keen, E. M. 2015. Net savvy: a practical guide to zooplankton sampler design. NOAA Technical Memoranda. NOAA-TM-NMFS-SWFSC-545.

Keen, E. M. 2017*a*. Whales of the rainforest: habitat use strategies of sympatric rorqual whales within a fjord system. Dissertation. University of California, San Diego, La Jolla, California, USA.

Keen, E. M. 2017*b*. The Bangarang Project. UC San Diego Library Digital Collections, University of California, San Diego, California, USA. https://doi.org/10.6075/J0MK69TN

Keen, E. M., K. B. Watson, K. M. Qualls, and R. Keen. 2016. A handheld rangefinder for seabird surveys within confined channels. Marine Ornithology 44:137–144.

Keen, E. M., J. Wray, H. Meuter, K. L. Thompson, J. P. Barlow, and C. R. Picard. 2017. "Whale wave": Shifting strategies structure the complex use of critical fjord habitat by humpbacks. Marine Ecology Progress Series, *in press*.

Laidre, K. L., M. P. Heide-Jorgensen, P. Heagerty, A. Cossio, B. Bergstrom, and M. Simon. 2010. Spatial associations between large baleen whales and their prey in West Greenland. Marine Ecology Progress Series 402:269–284.

Leatherwood, S., and R. R. Reeves. 1983. The Sierra Club handbook of whales and dolphins. Tien Wah Press, Singapore, Singapore.

Levin, S. A. 1992. The problem of pattern and scale in ecology. Ecology 73:1943–1967.

Logerwell, E. A., and N. B. Hargreaves. 1996. The distribution of sea birds relative to their fish prey off Vancouver Island: opposing results at large and small spatial scales. Fisheries Oceanography 5: 163–175.

Lovvorn, J. R., S. E. De La Cruz, J. Y. Takekawa, L. E. Shaskey, and S. E. Richman. 2013. Niche overlap, threshold food densities, and limits to prey depletion for a diving duck assemblage in an estuarine bay. Marine Ecology Progress Series 476: 251–268.

Lovvorn, J. R., and M. P. Gillingham. 1996. Food dispersion and foraging energetics: a mechanistic synthesis for field studies of avian benthivores. Ecology 77:435–451.

MacDonald, R. W., B. D. Bornhold, and I. Webster. 1983. The Kitimat fjord system: an introduction. Canadian Technical Report in Hydrography and Ocean Sciences 18:2–13.

Manly, B. F. J. 1991. Randomization and Monte Carlo methods in biology. Chapman and Hall, London, UK.

Mayo, C. E., and M. K. Marx. 1990. Surface foraging behavior of the North Atlantic right whale, *Eubalaena glacilais* and associated zooplankton characteristics. Canadian Journal of Zoology 68: 2214–2220.

Mitchell, C. A., T. W. Custer, and P. J. Zwank. 1994. Herbivory on shoalgrass by wintering redheads in Texas. Journal of Wildlife Management 58:131–141.

Nichol, L. M., and J. K. B. Ford. 2011. Information relevant to the assessment of critical habitat for blue, fin, sei and North Pacific right whales in British Columbia. Research Document 2011/137. Canadian Science Advisory Secretariat, Ottawa, Canada.

Nolet, B. A., A. Gyimesi, and R. H. G. Klaassen. 2006. Prediction of bird-day carrying capacity on a staging site: a test of depletion models. Journal of Animal Ecology 75:1285–1292.

Notarbartolo-di-Sciara, G., M. Zanardelli, M. Jahoda, S. Panigada, and S. Airoldi. 2003. The fin whale, *Balaenoptera physalus* (L. 1758), in the Mediterranean Sea. Mammal Review 33:105–150.

Panigada, S., G. Pesante, M. Zanardelli, and S. Oehen. 2003. Day and night-time behaviour of fin whales

in the Western Ligurian Sea. Pages 466–471. Proceedings of the Conference on Oceans, September 22–26, 2003. Town and Country Hotel and Convention Center, San Diego, California, USA.

Parker, H. W., and M. Boseman. 1954. The basking shark (*Cetrorhinus maximus*) in winter. Proceedings of the Zoological Society of London 124:185–194.

Piatt, J. F. 1990. The aggregative response of common murres and Atlantic puffins to schools of capelin. Journal of Avian Biology 14:36–51.

Piatt, J. F., and D. A. Methven. 1992. Threshold foraging behavior of baleen whales. Marine Ecology Progress Series 84:205–210.

Pike, G. 1950. Stomach contents of whales caught off the coast of British Columbia. Fisheries Research Board Canadian Pacific Progress Report 83:27–28.

R Development Core Team. 2013. R: a language and environment for statistical computing. R Foundation for Statistical Computing, Vienna, Austria. https://www.r-project.org/

Ryan, C., B. McHugh, C. N. Trueman, R. Sabin, R. Deaville, C. Harrod, S. D. Berrow, and I. O'Connor. 2013. Stable isotope analysis of baleen reveals resources partitioning among sympatric rorquals and population structure in fin whales. Marine Ecology Progress Series 479:251–261.

Seitz, R. D., R. N. Lipcius, K. E. Knick, M. S. Seebo, W. C. Long, B. L. Brylawski, and A. Smith. 2008. Stock enhancement and carrying capacity of blue crab nursery habitats in Chesapeake Bay. Review of Fisheries Sciences 16:329–337.

Sims, D. W. 1999. Threshold foraging behaviour of basking sharks on zooplankton: Life on an energetic knife-edge? Proceedings of the Royal Society of London B: Biological Sciences 266:1437–1443.

Solomon, M. F. 1949. The natural control of animal populations. Journal of Animal Ecology 18:1–35.

Sponberg, A. F., and D. M. Lodge. 2005. Seasonal belowground herbivory and a density refuge from waterfowl herbivory for *Vallisneria americana*. Ecology 86:2127–2134.

Thompson, R. E. 1981. Oceanography of the British Columbia coast. Special Publications in Fisheries and Aquatic Sciences 56. Department of Fisheries and Oceans, Ottawa, Canada.

van Eerden, R. E. 1984. Waterfowl movements in relation to food stocks. Pages 84–100 *in* P. R. Evans, J. D. Goss-Custard, and W. G. Hale, editors. Coastal waders and wildfowl in winter. Cambridge University Press, Cambridge, UK.

Witteveen, B., R. Foy, K. Wynneand, and Y. Tremblay. 2008. Investigation of foraging habits and prey selection by humpback whales (*Megaptera novaeangliae*) using acoustic tags and concurrent fish surveys. Marine Mammal Science 24:516–534.

Wolanski, E., and W. M. Hamner. 1988. Topographically controlled fronts in the ocean and their biological influence. Science 241:177–181.

Wood, S. N. 2011. Fast stable restricted maximum likelihood and marginal likelihood estimation of semiparametric generalized linear models. Journal of the Royal Statistical Society: Series B (Statistical Methodology) 73:3–36.

Zuur, A. L., E. N. Ieno, N. J. Walker, A. A. Saveliev, and G. M. Smith. 2009. Mixed effects models and extensions in ecology with R. Springer, New York, New York, USA.

Supporting Information

Additional Supporting Information may be found online at: http://onlinelibrary.wiley.com/doi/10.1002/ecs2.1702/full